To the Graduate Council:

I am submitting herewith a thesis written by Tasha N. Fernandez entitled “Analytical Computation of Proper Orthogonal Decomposition Modes and n-width Approximations for the Heat Equation with Boundary Control”. I have examined the final electronic copy of this thesis for form and content and recommend that it be accepted in partial fulfillment of the requirements for the degree of Master of Science, with a major in Electrical Engineering.

Seddik Djouadi, Major Professor

We have read this thesis
and recommend its acceptance:

J. Douglas Birdwell

James J. Nutaro

Accepted for the Council:

Carolyn R. Hodges
Vice Provost and Dean of the Graduate School

Analytical Computation of Proper Orthogonal Decomposition Modes and n-Width Approximations for the Heat Equation with Boundary Control

A Thesis Presented for
the Master of Science
Degree
The University of Tennessee, Knoxville

Tasha N. Fernandez
December 2010

Copyright © 2010 by Tasha Fernandez
All rights reserved.

Acknowledgements

I would like to express my sincere appreciation to my advisor Dr. Seddik Djouadi for suggesting the topic of this thesis, and second, for his guidance, support, and patience. In addition, I would like to express my thanks to Dr. Don B. Hinton and Dr. Heather Finotti, of the mathematics department and Dr. A.J. Baker, director of the computational fluid dynamics laboratory, for taking the time to answer questions pertaining to my thesis.

I also wish to thank the Department of Energy for support under the Pipeline Diversity Engineering Program and its director, James Pippin.

Abstract

Model reduction is a powerful and ubiquitous tool used to reduce the complexity of a dynamical system while preserving the input-output behavior. It has been applied throughout many different disciplines, including controls, fluid and structural dynamics. Model reduction via proper orthogonal decomposition (POD) is utilized for of control of partial differential equations. In this thesis, the analytical expressions of POD modes are derived for the heat equation. The autocorrelation function of the latter is viewed as the kernel of a self adjoint compact operator, and the POD modes and corresponding eigenvalues are computed by solving homogeneous integral equations of the second kind. The computed POD modes are compared to the modes obtained from snapshots for both the one-dimensional and two-dimensional heat equation. Boundary feedback control is obtained through reduced-order POD models of the heat equation and the effectiveness of reduced-order control is compared to the full-order control. Moreover, the explicit computation of the POD modes and eigenvalues are shown to allow the computation of different n-widths approximations for the heat equation, including the linear, Kolmogorov, Gelfand, and Bernstein n-widths.

Table of Contents

Chapter 1 Introduction 1
Background 1
Problem Statement 6
Thesis Overview 8
Chapter 2 Proper Orthogonal Decomposition Method 9
Optimality 10
Method of Snapshots 13
Analytical Computation Method 14
Chapter 3 Model Reduction for the Heat Equation 22
The One-Dimensional Heat Equation 22
The Two-Dimensional Heat Equation 33
Chapter 4 Boundary Feedback Control 41
LQR Control Law Design 41
The One-Dimensional Heat Equation 44
The Two-Dimensional Heat Equation 47
Chapter 5 Model Reduction and N-Width Approximations 50
Chapter 6 Conclusion and Future Work 57
List of References 61
Vita 67

List of Figures

Figure 1. POD modes for the one-dimension problem 28
Figure 2. POD modes from method of snapshots 29
Figure 3. Model comparison for the one-dimension problem 31
Figure 4. Comparison of full-order and analytical POD temporal coefficients 32
Figure 5. Two-Dimensional Problem Geometry 33
Figure 6. POD modes for the two-dimensional problem 37
Figure 7. Full-order simulation 38
Figure 8. Reduced-order simulation 38
Figure 9. Projected and POD model coefficients 39
Figure 10. Controlled three-mode analytical POD model 45
Figure 11. Full order Control 46
Figure 12. Reference function from a eight-mode projection 48
Figure 13. Steady-state controlled eight-mode POD model 48

Chapter 1

Introduction

Background

Recently significant interest and research efforts have been focused on feedback control law design for physical high-dimensional systems described by partial differential equations (PDEs) [1]-[12]. For example, feedback control can enable the use of controllers to stabilize an unstable system and ensure satisfactory performance despite modeling errors. In many situations, a very large number of states are needed to accurately capture the dynamics of the input-output system but are unsuitable for feedback control design [1]-[3],[6]-[13]. Conventionally the order of the system must be reduced before control law design can be performed [6]. Control of PDEs normally comes in two settings: “in domain” control, where the actuation penetrates inside the domain or is evenly distributed everywhere in the domain and “boundary” control, where actuation is applied only through the boundary conditions. Boundary control is generally considered the more realistic problem called for by many of the current applications [2][6][9][12]. For example, in [2][9][12][13], the authors designed boundary feedback controllers based on reduced-order models obtained using a combination of model reduction techniques such as balanced truncation [12], POD [2][9] and Hankel norm [13]. Each paper’s approach was applied to the

two-dimensional Burger's equation and presented favorable results and excellent tracking.

Reduced-order modeling is a powerful and ubiquitous tool and has been given significant attention in recent years. Additions to literature in this area seem to be continuing [1]-[16]. Research in the area of reduced-order modeling has followed two avenues: non-projection based and projection based. Hankel-norm model reduction is an example of a non-projection based model reduction technique. Some of the early work on this technique by Glover and Kung [14]-[16] was concerned with approximating a transfer function, G, of degree n by a reduced G_r of degree $r < n$ via the induced-norm of the associated hankel operators. In [13] the authors developed an empirical Hankel norm model reduction algorithm where an empirical balancing transformation was used with minimal computational effort. Application to a nonlinear convective flow problem with excellent results was proposed. The vast majority of research is concerned with projection based methods, such as balanced truncation and POD. Several papers on these methods address applications in physics and fluid mechanics, particularly aerodynamic flow control [1]-[13]. In [6], weak formulations of POD system models were obtained for a system described by the two-dimensional heat equation on a geometry most often seen in cavity noise reduction applications. The feedback controllers were able to satisfy tracking objectives of POD models consisting of three modes or less.

POD for reduced-order modeling is a well established area of research. Indeed, there is a large body of literature on POD and many impressive results have been obtained for various applications. POD was developed by several people, including Kosamibi [28], Loéve [29], and Karhunen [30]. POD is also known as Principal Component Analysis, the Karhunen-Loeve Decomposition, and the singular value decomposition. POD has been used to obtain approximate reduced-order models of turbulent flows [4], structural vibrations [31], and has been used for flow control [2][5]-[9][11]-[13], to name a few applications in dynamic systems. POD has been traditionally formulated to reduce the dimensionality of a data set in which there are a large number of interrelated variables, while retaining as much as possible of the variation present in the data set [32]. Often, its operation can be thought of as obtaining low-dimensional descriptions that capture much of the phenomena of interest. POD's most notable property is *optimality* in an energy sense and therefore it can provide an efficient way of accurately capturing the dominant behavior of systems of an *infinite*-dimensional process with only *finitely* many, and often surprisingly few, "modes" [4]. Normally, POD is performed to extract "mode shapes" or basis functions from data obtained in the course of experiments or simulation known as the method of snapshots [4]. The method of snapshots was originally suggested by Sirovich as a way to reduce the computational effort in solving the eigenvalue problem necessary for the POD [4][33].

The tools of POD along with Galerkin projection have been used for some time as a model order reduction technique by converting an infinite-dimensional partial differential equation into a finite set of ordinary differential equations [1]-[13][18][20]. Galerkin projection results in only a weak solution to the PDE [18][20]. However, this weak formulation with the boundary conditions eventually leads to a temporal POD model. POD models such as these of only a few dozen states have been shown to accurately capture the system dynamics of the full-order system model of thousands of states [5]. Moreover, POD models have been shown to construct a new reduced-order state-space representation of the physical system to be used to design feedback control laws [2]-[13]. Many practical problems, including those of interest in the fluid mechanics community, require that the control be located on a domain boundary. Boundary feedback control design from reduced-order POD models has been applied to many problems, for example, to nonlinear two-dimensional convection [2]-[13].

Reduced-order modeling can be divided into two stages consisting of information acquisition and information processing and also can be formulated as input design and model selection problem [37]. Model reduction should accurately and efficiently identify a reduced-order model with the least number of states possible while keeping the representation within a given error tolerance. This estimation error can be split into two parts, the *inherent* and *representation* errors. The optimal inherent and representation error can be quantified in terms of various n-

widths. The idea of the link between optimal identification error and so-called ε-entropy was first introduced in control by Zames [34] using metric complexity theory. N-widths have seen a great deal of work over the years by a variety of mathematicians: Kolmogorov, Gel'fand, Tikhomirov, Kashin, Gluskin, etc. There are many different n-widths. The book by Pinkus [27] is a good reference on n-widths approximations. N-widths can be utilized to quantify the representation and inherent errors in model reduction. The role of POD and balanced truncation in minimizing different n-widths of specific compact operators was pointed out in [10].

Some of the material of this thesis has been accepted for publication [35].

Problem Statement

In this thesis, we will introduce and illustrate the analytical computation of the POD modes for the model reduction of a system described by the heat equation. The empirical computation of the POD modes by the method of snapshots for the heat equation was first introdcued in [6]. This thesis uses the results of that paper for model development and comparison.

The optimal basis or POD modes are given by the eigenfunctions of a homogeneous integral equation whose kernel, a self-adjoint compact operator, is the autocorrelation function. The autocorrelation function is defined as

$$R(\boldsymbol{x}, \boldsymbol{x}') = \int_0^T w(t, \boldsymbol{x}) w(t, \boldsymbol{x}') dt \qquad 1.1$$

where $w(t, \boldsymbol{x})$ is the solution to the PDE. Formerly, Sirovich's method of snapshots has been widely used as a way of determining these basis functions without explicitly calculating the kernel (1.1) [1][4][5].

There are many powerful analytical techniques for solving a variety of linear partial differential equations, particularly Galerkin projection. Separation of variables is a good tool for solving linear PDEs but Galerkin projection is better at handling various types of boundary conditions. For linear PDEs, an approximate solution can be generated as a linear combination of a set of suitable basis

functions and a set of unknown expansion coefficients to be determined as part of the solution process. Instead of performing a set of simulations to obtain the snapshots, the POD basis functions can be analytically computed using the approximate solutions found for the partial differential equations. However, an analytic solution of a partial differential equation needs to be available. In general, analytic solutions to PDEs are hard to compute or do not exist. This limits our method to PDEs defined on favorable geometries without boundary singularities [20].

Empirical and analytical expressions of the POD modes are derived for specific partial differential equation. The computed POD modes are compared to the modes obtained from the snapshot method which uses simulation data. The method is illustrated on prototype problems which involve the one- and two-dimensional heat equations with boundary control. Model reduction results are compared to full-order models. A new reduced-order state-space model is formed by a Galerkin projection of the governing equations and initial conditions onto the POD basis. The techniques of boundary feedback control laws based on linear quadratic regulator (LQR) control formulation is developed from the weak formulation of POD models as presented in [6]. Later, we show that the analytic expressions of the POD modes and eigenvalues allow the computation of different n-widths approximations for the heat equation, including the time, linear, Kolmogorov, Gel'fand, and Bernstein n-widths.

Thesis Overview

Chapter 2 introduces the existing concepts of proper orthogonal decomposition (POD) and discusses the empirical computation by way of Sirovich's method of snapshots and the analytical computation of the POD modes for systems described by partial differential equations.

Chapter 3 extends the techniques of chapter 2 to find the analytical POD model for prototype problems which involve the one- and two-dimensional heat equations. Results from the method of snapshots and solving the modes analytically are compared.

Chapter 4 presents the design methodology for the linear-quadratic regulator controller using the boundary feedback control laws for the resultant finite-dimensional system described by the heat equation.

Chapter 5 introduces the concept of n-widths of various types and how they relate to error in approximating lower order finite-dimensional models for a given input.

Chapter 6 briefly summarizes the thesis contributions, and recommendations for future research. Selected references are included at the end of the thesis.

Chapter 2

Proper Orthogonal Decomposition Method

The central idea of proper orthogonal decomposition is to extract from experimental data or simulations a “relevant” set of optimal basis functions from which we can identify low-dimensional descriptions of high-dimensional systems. The fundamental idea behind the POD is simple but not straightforward.

Suppose we wish to approximate the solution of the partial differential equation $w(t, \boldsymbol{x})$ over some domain of interest as a finite sum of the form

$$w(t, \boldsymbol{x}) \approx \sum_{j=1}^{N} a_j(t)\varphi_j(\boldsymbol{x}) \tag{2.1}$$

where t is time and $\boldsymbol{x}$ is the spatial coordinate with the reasonable expectation that the approximation becomes exact in the limit as N approaches infinity. We assume that the function $w(t, \boldsymbol{x})$ is finite energy, and therefore belongs to the Hilbert space $L^2([0, T) \times \Omega)$ of Lebesque measurable and square integrable functions under the norm [4][10]

$$\|w(t, \boldsymbol{x})\|_2 \stackrel{\text{def}}{=} \sqrt{\int_0^T \int_\Omega |w(t, \boldsymbol{x})|^2 dx dt} < \infty \tag{2.2}$$

where T represents a finite or infinite time interval, and Ω represents the problem geometry. The corresponding inner product is given by

$$(f,g)=\int_0^T\int_\Omega f(t,\boldsymbol{x})g^*(t,\boldsymbol{x})d\boldsymbol{x}dt \tag{2.3}$$

for some functions f and g. The representation of eq. (2.1) is not unique. For each choice of a sequence $\{\varphi_j(\boldsymbol{x})\}_{j=1}^{\infty}$ that forms a basis for the function $w(t,\boldsymbol{x})$, the sequence of temporal functions $a_j(t)$ is different. The POD is concerned with one possible optimal choice of the functions $\{\varphi_j(\boldsymbol{x})\}_{j=1}^{\infty}$.

Optimality

The basis functions φ are chosen to maximize the average projection of $w(t,x)$ onto φ:

$$\max_{\varphi\in L^2(\Omega)}\frac{\langle|(w,\varphi)|^2\rangle}{\|\varphi\|_2{}^2} \tag{2.4}$$

where $|\cdot|$ denotes the modulus, $\langle\cdot\rangle$ represents a time-averaging operation and $\|\cdot\|_2$ is the L^2 norm [4]. In [10] it is shown that the approximation eq. (2.1) can be as accurate as desired since the tensor space

$$L^2([0,T))\otimes L^2(\Omega)\stackrel{\text{def}}{=}\sum_{j=1}^{N}a_j(t)\phi_j(\boldsymbol{x}),a_j(t)\in L^2\big([0,T)\big),\quad \phi_j(\boldsymbol{x})\in L^2(\Omega) \tag{2.5}$$

is dense in L^2. This implies that in the limit in the L^2-norm (i.e. limit in the mean (l.i.m.)) we have that

$$w(t,x) \underset{l.i.m.}{=} \sum_{j=1}^{\infty} a_j(t)\varphi_j(\boldsymbol{x}) \tag{2.6}$$

where the POD basis $\{\phi_j\}$ are optimal in the following sense [17]

$$\mu_n \overset{\text{def}}{=} \inf_{\substack{a_k \in L^2([0,T)) \\ \phi_k(\boldsymbol{x}) \in L^2(\Omega)}} \left\| w(t,\boldsymbol{x}) - \sum_{k=1}^{N} a_j(t)\varphi_j(\boldsymbol{x}) \right\|_2 \tag{2.7}$$
$$\mu_n \underset{n\to\infty}{\longrightarrow} 0$$

In [10] it is shown that solving the above optimization, eq. (2.7), reduces to the usual POD optimality in the average kinetic energy sense as discussed in [4]. The optimal POD basis is given by the eigenfunctions $\{\varphi_j\}$ of an integral equation whose kernel is the autocorrelation function, denoted $R(\boldsymbol{x},\boldsymbol{x}')$, of the PDE solution, that is, [4]

$$\int_{\Omega} R(\boldsymbol{x},\boldsymbol{x}')\,\varphi(\boldsymbol{x}')d\boldsymbol{x}' = \lambda\varphi(\boldsymbol{x}) \tag{2.8}$$

where

$$R(\boldsymbol{x},\boldsymbol{x}') \overset{\text{def}}{=} \int_0^T w(t,\boldsymbol{x})w(t,\boldsymbol{x}')dt \tag{2.9}$$

Note that since $w(t,\boldsymbol{x})$ is assumed to belong to $L^2([0,T)\times\Omega)$ the autocorrelation function $R(\boldsymbol{x},\boldsymbol{x}') \in L^2(\Omega\times\Omega)$, the Hilbert space of square integrable functions of functions defined over the spatial domain $\Omega\times\Omega$. The self adjoint compact operator $\boldsymbol{R}$ with kernel, $R(\boldsymbol{x},\boldsymbol{x}')$, is defined as

$$(\boldsymbol{R}\phi)(x) = \int_{\Omega} R(\boldsymbol{x},\boldsymbol{x}')\,\phi(\boldsymbol{x}')d\boldsymbol{x}', \quad \phi \in L^2(\Omega) \tag{2.10}$$
$$\boldsymbol{R}: L^2(\Omega\times\Omega) \to L^2(\Omega)$$

where $L^2(\Omega)$ is the Hilbert space of square integrable functions defined on Ω. The eigenvalue problem then becomes.

$$\boldsymbol{R}\phi = \lambda\phi, \quad \phi \in L^2(\Omega) \tag{2.11}$$

By the spectral theorem compactness of $\boldsymbol{R}$ implies that the eigenvalue problem has infinitely countable eigenvalues, λ, and eigenfunctions, ϕ [17]. That is there is a sequence $\{\lambda_i\}$ of non-zero eigenvalues of $\boldsymbol{R}$ and a corresponding orthonormal sequence $\{\varphi_i\}$ of eigenvectors such that for each $\phi \in L^2(\Omega)$

$$\boldsymbol{R}\phi = \sum_{i=0}^{\infty} \lambda_i(\phi, \varphi_i)\varphi_i \tag{2.12}$$

where $(\cdot,\cdot)$ denotes the inner product in $L^2(\Omega)$, $\lambda_i \to 0$ as $i \to \infty$ and in fact

$$\sum_{i=1}^{\infty}|\lambda_i|^2 < \infty, \quad \varphi_i \in L^2(\Omega) \tag{2.13}$$

Therefore **R** is a Hilbert-Schmidt operator. To solve the eigenvalue problem we need to reduce it to a finite-dimensional problem and then invoke a limit argument. This can be achieved by defining

$$\boldsymbol{R}_N\phi = \sum_{i=0}^{\infty} \lambda_i(\phi, \varphi_i)\varphi_i \tag{2.14}$$

then $\|\boldsymbol{R} - \boldsymbol{R}_N\|_2 \to 0$ as $N \to \infty$ [18] and if $R_N(\boldsymbol{x}, \boldsymbol{x}')$ is the corresponding kernel we have that [17]

$$\int_{\Omega}\int_{\Omega} |R(\boldsymbol{x}, \boldsymbol{x}') - R(\boldsymbol{x}, \boldsymbol{x}')|^2 d\boldsymbol{x}d\boldsymbol{x}' \to 0 \; as \;\; N \to \infty \tag{2.15}$$

Since the spectral decomposition is unique the spectral factorization of the finite rank operator $\boldsymbol{R}_N$ converges to its infinite dimensional counterpart R.

Method of Snapshots

Sirovich introduced the method of snapshots as a way of determining the eigenfunctions $\varphi(\boldsymbol{x})$ without explicitly calculating the kernel R necessary for POD [1][4][33]. The kernel can be approximated by starting with an ensemble of solution snapshots $\{S_i(\boldsymbol{x})\}_{i=1}^{N}$, or system states at time t with nontrivial input data and the number of snapshots N is sufficiently large [1][6]. To numerically compute the POD basis we construct the $N \times N$ correlation matrix L composed of the inner product of the snapshots:

$$L_{i,j} = \left(S_i, S_j\right) \tag{2.16}$$

where $(\cdot,\cdot)$ denotes the $L^2(\Omega)$ inner product defined as

$$\left(S_i, S_j\right) = \int_{\Omega} S_i {S_j}^* \, d\boldsymbol{x} \tag{2.17}$$

where ${S_j}^*$ denotes the complex conjugate of S_j, in the construction of L. The eigenvalues, $\{\lambda_i\}$, of L are found and sorted in descending order and their corresponding eigenvectors, $\{v_i\}$, are calculated. Each eigenvector is normalized so that [6]

$$\|v_i\|^2 = \frac{1}{\lambda_i} \tag{2.18}$$

The orthonormal POD basis set, namely the eigenvectors of the kernel, is created according to

$$\varphi_i(\boldsymbol{x}) = \sum_{j=1}^{N} v_{j,i} S_j(\boldsymbol{x}) \tag{2.19}$$

which is the linear combination of the normalized eigenvectors and the snapshots where $v_{j,i}$ is the ith component of v_j [6]. Solving eq. (2.19) gives n vectors φ_i's, which constitute the POD basis of dimension n. As the POD modes form an optimal basis for the snapshots in the energy sense, the solution $w(t, \boldsymbol{x})$ is approximated by a linear combination of the POD basis functions as

$$w(t, \boldsymbol{x}) \approx \sum_{j=1}^{N} a_j(t) \varphi_j(\boldsymbol{x}) \tag{2.20}$$

which is the linear combination of the POD modes and a set of unknown temporal coefficients $a_j(t)$.

Analytical Computation Method

Rather than performing a set of simulations to obtain the solution snapshots, the POD modes can be obtained analytically. To begin we approximate the PDE solution $w(t, \boldsymbol{x})$ over Ω as a finite sum (note this approximation can be as accurate as needed)

$$w(t, \boldsymbol{x}) \approx \sum_{j=1}^{N} a_j(t) \varphi_j(\boldsymbol{x}) \tag{2.21}$$

The finite-dimensional version of the POD is solved as an eigenvalue problem. It can be shown that a necessary condition for eq. (2.4) to hold is that φ is an eigenfunction of the following integral equation

$$\int_{\Omega} R(\boldsymbol{x}, \boldsymbol{x}')\varphi(\boldsymbol{x}')d\boldsymbol{x}' = \lambda\varphi(\boldsymbol{x}) \tag{2.22}$$

whose kernel is the averaged autocorrelation function defined by (2.9)

$$R(\boldsymbol{x}, \boldsymbol{x}') = \int_{0}^{T} w(t, \boldsymbol{x})w^{*}(t, \boldsymbol{x}')dt \tag{2.23}$$

where $\boldsymbol{x}$ and $\boldsymbol{x}'$ are spatial vectors belonging to domain Ω [4]. Eq. (2.22) is a homogeneous Fredholm integral equation of the second kind where the function $\varphi(\boldsymbol{x})$ represents the unknown POD modes.

Solving for the POD modes analytically requires finding the kernel (2.23) which can easily be found using the approximate solution to the partial differential equation. Once found the kernel is placed into the integral equation (2.22) to solve for the POD modes $\varphi(\boldsymbol{x})$. Since the PDE solution $w(t, \boldsymbol{x})$ is assumed be finite energy, i.e., belongs to the Hilbert space $L_2([0, T) \times \Omega)$ and can be approximated as a finite sum of time-dependent modal coefficients multiplied by elements of a known suitable orthonormal basis functions $\psi_j(\boldsymbol{x})$ it can be defined as

$$w(t, \boldsymbol{x}) \approx \sum_{j=1}^{N} b_j(t)\psi_j(\boldsymbol{x}) \tag{2.24}$$

where $\{\psi_j\}$ is any basis for $L^2(\Omega)$.

Galerkin projection can be performed to determine the unknown expansion coefficients $b_j(t)$. The sum in eq. (2.24) substituted into the kernel (2.23) results in

$$R(\boldsymbol{x},\boldsymbol{x}') = \int_0^T w(t,\boldsymbol{x})w^*(t,\boldsymbol{x}')dt = \int_0^T \sum_{j=1}^{N} b_j(t)\psi_j(\boldsymbol{x}) \sum_{k=1}^{N} b_k(t)\psi_k(\boldsymbol{x}')\,dt$$
$$= \sum_{j=1}^{N}\sum_{k=1}^{N} \int_0^T b_j(t)b_k(t)dt\,\psi_j(\boldsymbol{x})\,\psi_k(\boldsymbol{x}') \qquad 2.25$$

where $\int_0^T b_j(t)b_k(t)dt = b_{jk}$. The kernel $R(\boldsymbol{x},\boldsymbol{x}')$ is separable and symmetric and with such a kernel, the homogeneous Fredholm integral equation of the second kind becomes

$$\lambda\varphi(\boldsymbol{x}) = \sum_{j=1}^{N}\sum_{k=1}^{N} b_{jk}\psi_j(\boldsymbol{x}) \int_\Omega \psi_k(\boldsymbol{x})\varphi(\boldsymbol{x}')d\boldsymbol{x}' \qquad 2.26$$

It emerges that the technique of solving this equation is essentially dependent on the choice of the complex parameter λ and on the definition of

$$c_k = \int_\Omega \psi_k(\boldsymbol{x})\varphi(\boldsymbol{x}')d\boldsymbol{x}' \qquad 2.27$$

The coefficients c_k are constants but unknown. Substituting eq. (2.23) into eq. (2.22) gives

$$\lambda\varphi(\boldsymbol{x}) = \sum_{j=1}^{N}\sum_{k=1}^{N} b_{jk}\psi_j(\boldsymbol{x})\,c_k \qquad 2.28$$

and the problem reduces to finding the $c_k's$. Taking the inner product on both sides of eq. (2.28) with $\psi_i(\boldsymbol{x})$ yields

$$\lambda \int_\Omega \psi_i(\boldsymbol{x})\varphi(\boldsymbol{x})\, d\boldsymbol{x} = \lambda c_i = \sum_{j=1}^{N}\sum_{k=1}^{N} b_{jk}\, c_k \int_\Omega \psi_i(\boldsymbol{x})\psi_j(\boldsymbol{x})\, d\boldsymbol{x} \qquad 2.29$$

and due to the orthonormality of $\psi_i(\boldsymbol{x})$ reduces to

$$\lambda c_i = \sum_{k=1}^{N} b_{ik}\, c_k \qquad 2.30$$

The problem presented by eq. (2.30) is one we can solve, the usual theory of matrices where c is the eigenvectors with corresponding eigenvalues λ of the $N \times N$ matrix whose (i,k)- th entry is b_{ik}.

Next, the eigenvalues $\{\lambda_i\}$ are sorted in descending magnitude. The ratio

$$100\left(\frac{\sum_{i=1}^{M}\lambda_i}{\sum_{i=1}^{N}\lambda_i}\right) \qquad 2.31$$

can be utilized to determine the number of POD basis functions to construct [12]. The quantity in eq. (2.31) provides a measure of the ensemble energy that is captured by a POD basis consisting of M modes [12]. The eigenvectors $\{c_i\}$ corresponding to the M eigenvalues of the largest magnitude are used to construct the orthonormal POD basis set as

$$\varphi_i(\boldsymbol{x}) = \sum_{j=1}^{N} c_{j,i}\psi_j(\boldsymbol{x}) \qquad 2.32$$

where $c_{j,i}$ is the ith component of c_j and $\psi_j(\boldsymbol{x})$ is a suitable basis function to solve the partial differential equation. The solution $w(t,\boldsymbol{x})$ can now be rewritten in terms of the POD modes as

$$w(t,\boldsymbol{x}) \approx \sum_{j=1}^{N} a_j(t)\varphi_j(\boldsymbol{x}) \tag{2.33}$$

The temporal coefficients $\{a_j\} \subseteq L^2([0,T))$, and the sequence $\{a_j\}$ form a basis for $L^2([0,T))$. Moreover [4],

$$a_j(t) = \int_{\Omega} w(t,\boldsymbol{x})\,\varphi_j(x)d\boldsymbol{x} \tag{2.34}$$

Next, we extend the technique to solve for the POD modes to the two-dimensional case. For the two-dimensional case the approximate solution to the partial differential equation can also be written as a finite sum

$$w(t,x,y) \approx \sum_{i=1}^{N}\sum_{j=1}^{N} b_{ij}(t)\psi_{ij}(x,y) \tag{2.35}$$

where $t > 0$, $(x,y) \in (\Omega \times \Omega)$ and ψ_{ij} is any basis function for $L^2(\Omega \times \Omega)$. The kernel for the two-dimensional problem becomes

$$R(x,x',y,y') = \sum_{i=1}^{N}\sum_{j=1}^{N}\sum_{n=1}^{N}\sum_{m=1}^{N} b_{ijnm}\psi_{ij}(x,y)\,\psi_{nm}(x',y') \tag{2.36}$$

which is symmetric and separable. The two-dimensional POD basis, like the one-dimensional case, is found using a homogeneous Fredholm integral equation of the second kind of the form

$$\int_{\Omega}\int_{\Omega} R(x,x',y,y')\varphi(x',y')\,dx'dy' = \lambda\varphi(x,y) \tag{2.37}$$

Substituting (2.32) into eq. (2.33) and following the same steps outlined for the one-dimensional case above reduces the integral equation (2.33) to

$$\lambda c_{rl} = \sum_{n=1}^{N}\sum_{m=1}^{N} b_{rlnm}c_{nm} \tag{2.38}$$

Eq. (2.38) simplifies to the usual theory of matrices where c is the eigenvectors with corresponding eigenvalues λ of the $N \times N$ matrix whose (i,j)- th entry is b_{ijnm}. Sorting the eigenvalues and their corresponding eigenvectors in descending magnitude constructs the orthonormal two-dimensional POD basis set as

$$\varphi_i(x,y) = \sum_{j=1}^{N}\sum_{k=1}^{N} c_{jk,i}\,\psi_{jk}(x,y) \tag{2.39}$$

where $c_{jk,i}$ is the ith component of c_{jk}. In terms of the POD modes the solution is

$$w(t,x,y) = \sum_{i=1}^{N}\sum_{j=1}^{N} a_{ij}(t)\varphi_{ij}(x,y) \tag{2.40}$$

Moreover, to simplify the complexity of eq. (2.40) or the number of index variables, one can make a change of variable with the following transformation: let us define

$$\beta_j(t) = \begin{bmatrix} b_{11}(t) \\ b_{12}(t) \\ \vdots \\ b_{ij}(t) \end{bmatrix} \tag{2.41}$$

and

$$\Psi_j(x,y) = \begin{bmatrix} \psi_{11}(x,y) \\ \psi_{12}(x,y) \\ \vdots \\ \psi_{ij}(x,y) \end{bmatrix} \tag{2.42}$$

Therefore eq. (2.40) can be rewritten as

$$w(t,x,y) \approx \sum_{j=1}^{N^2} \beta_j(t)\Psi_j(x,y) \tag{2.43}$$

and note that the upper bound of summation changes from N to N^2. Using eq. (2.43), finding the analytical POD modes will be similar to the method used for the one-dimensional case. To illustrate, the kernel simplifies to

$$R\left(x,x',y,y'\right) = \sum_{j=1}^{N^2}\sum_{k=1}^{N^2} \beta_{jk}\Psi_j(x,y)\,\Psi_k(x',y') \tag{2.44}$$

Plugging eq. (2.44) into the integral equation (2.37) yields

$$\sum_{j=1}^{N^2}\sum_{k=1}^{N^2} \beta_{jk}\,\Psi_j(x,y) \int_{\Omega}\int_{\Omega} \Psi_k(x',y')\varphi\left(x',y'\right)dx'dy' = \lambda\varphi(x,y) \tag{2.45}$$

Taking the inner product of both sides of eq. (2.45) with $\Psi_i(x,y)$ reduces it to

$$\lambda c_i = \sum_{k=1}^{N^2} \beta_{ik}\,c_k \tag{2.46}$$

Both methods for solving for the POD modes produce an approximate solution as a linear combination of the POD basis functions and a set of unknown temporal coefficients. To solve for the temporal coefficients the next step is to take the governing equation and its initial condition and project them onto the POD basis via Galerkin projection. The Galerkin projection results in a weak solution to the PDE. However, this weak formulation with the boundary conditions gives a system of ordinary differential equations (ODEs) for the temporal or POD coefficients $a(t)$ [12]. Solving for the a's creates a convenient state-space representation of the form

$$\dot{a}(t) = Aa(t) + Bu(t) \qquad 2.47$$

where $a(t) \in \Re^n$ and the matrices A is $N \times N$ and B is $N \times m$, where m is the number of inputs and this is used to develop the reduced-order POD model. The order reduction method just described results in a model that can be simulated much more efficiently than the original full-order system.

In this chapter, the methods to solve for the POD basis modes empirically and analytically were discussed. In the next chapter, both procedures will be applied to the one-dimensional and two-dimensional heat equation to obtain reduced-order models and the results will be compared.

Chapter 3

Model Reduction for the Heat Equation

We are now ready to illustrate the techniques discussed by finding a reduced-order model using the analytical POD modes for both the one-dimensional and two-dimension heat equation. The heat equation is an important partial differential equation which describes the distribution of heat (or variation in temperature) in a given region over time.

The One-Dimensional Heat Equation

The one-dimensional heat equation on a unit interval (or rod) is described by

$$w_t(t,x) = \varepsilon w_{xx}(t,x), \;\; t > 0, \;\; x \in (0,1) \tag{3.1}$$

with initial conditions

$$w(0,x) = w_0(x) \tag{3.2}$$

and by requiring Dirichlet boundary control, the time-dependent boundary conditions are specified as

$$w(t,0) = u_0(t) \tag{3.3}$$

$$w(t,1) = u_1(t) \tag{3.4}$$

where $u_0(t)$ is the time-dependent control at $x = 0$ and $u_1(t)$ is the time-dependent control at $x = 1$.

We assume that the solution to eq. (3.1) be finite energy, i.e., belongs to the Hilbert space $L^2([0,T)\times\Omega)$ and can be approximated as a finite sum

$$w(t,x) \approx \sum_{j=1}^{N} b_j(t)\psi_j(x) \qquad 3.5$$

where the $\{\psi_j(x)\}$ functions are a set of known orthonormal functions defined over the domain of interest and the $\{b_j(t)\}$ functions are the unknown time-varying coefficients to be determined as part of the solution process. Due to the time-dependent inhomogeneous boundary conditions, (3.3-3.4), the usual method of separation fails and therefore Galerkin projection is performed to completely define a set of first order linear ordinary differential equations (ODEs) for the $\{b_j(t)\}$ coefficients. Given $u_0(t)$ and $u_1(t)$ for a particular problem, this system can be solved for the specific time-dependent coefficients of interest. These coefficients, coupled with the spatial functions defined by the known orthonormal basis functions give the final solution to the problem via (3.5).

To illustrate this method, taking the inner product of both sides of eq. (3.1) with $\{\psi_k(x)\}$ yields

$$\int_0^1 w_t(t,x)\psi_k(x)\,dx = \varepsilon \int_0^1 w_{xx}(t,x)\psi_k(x)\,dx \qquad 3.6$$

Integrating the right hand side of this expression by parts twice gives

$$\int_0^1 w_t(t,x)\psi_k(x)\,dx$$

$$= \varepsilon\left[w_x(t,x)\psi_k(x)|_0^1 + w(t,x)\frac{\partial\psi_k(x)}{\partial x}\Big|_1^0 + \int_0^1 w\frac{\partial^2\psi_k(x)}{\partial x^2}dx\right] \quad 3.7$$

The boundary conditions are made explicit by replacing $w(t,0)$ and $w(t,1)$. Substituting the boundary conditions into eq. (3.7) and writing $w(t,x)$ as a linear combination of the orthonomal basis function results in

$$\dot{b_j}(t) = 2\varepsilon\left[u_0(t)\frac{\partial\psi_k(0)}{\partial x} - u_1(t)\frac{\partial\psi_k(1)}{\partial x} + \sum_{j=1}^{N} b_j(t)\int_0^1 \psi_j(x)\frac{\partial^2\psi_k(x)}{\partial x^2}dx\right] \quad 3.8$$

In the results that follow, the initial condition specified is $w_0(x) = \sin\pi x$. The value for the conductivity constant is $\varepsilon = 0.1$. For this example, we chose the suitable basis functions to solve for the heat equation to be $\{\sin j\pi x\}_{j=1}^{N}$ and specify the control inputs to be open-loop and time-varying. The values for the control inputs are $u_0(t) = \sin\pi t$ and $u_1(t) = \sin\pi t$. Orthogonality of the basis functions simplifies the ODE in eq. (3.8) to

$$\dot{b_j}(t) = -\varepsilon j^2\pi^2 b_j(t) + 2\varepsilon j\pi\sin\pi t - 2\varepsilon j\pi(-1)^j\sin\pi t \quad 3.9$$

These may be solved immediately to yield

$$b_j(t) = \frac{4\varepsilon j\pi}{\pi^2 + (\varepsilon j^2\pi^2)^2}(\varepsilon j^2\pi^2\sin\pi t - \pi\cos\pi t) + C_j e^{-\varepsilon j^2\pi^2 t}, j = 1,3,5\ldots \quad 3.10$$

in which the coefficients C_j are determined by taking the inner product of eq. (3.5) with $\psi_k(x)$ at $t = 0$.

$$b_j(0) = 2\int_0^1 w(0,x)\psi_k(x)\,dx = 2\int_0^1 \sin\pi x \sin \mathrm{k}\pi \mathrm{x}\,dx \qquad 3.11$$

With this result, we have a complete set of expressions that define the expansion coefficients for $w(t,x)$.

$$w(t,x) \approx b_1(t)\sin \pi \mathrm{x} + \sum_{\substack{j=3 \\ odd}}^{N} b_j(t)\sin j\pi \mathrm{x} \qquad 3.12$$

where

$$b_1(t) = \frac{4\varepsilon\pi}{\pi^2 + (\varepsilon\pi^2)^2}(\varepsilon\pi^2 \sin\pi t - \pi\cos\pi t) + \left(1 + \frac{4\varepsilon\pi^2}{\pi^2 + (\varepsilon\pi^2)^2}\right)e^{-\varepsilon\pi^2 t} \qquad 3.13$$

$$b_j(t) = \frac{4\varepsilon j\pi}{\pi^2 + (\varepsilon j^2\pi^2)^2}(\varepsilon j^2\pi^2 \sin\pi t - \pi\cos\pi t) + \frac{4\varepsilon j\pi^2}{\pi^2 + (\varepsilon j^2\pi^2)^2}e^{-\varepsilon j^2\pi^2 t} \qquad 3.14$$

In the limit the solution is

$$w(t,x) \underset{l.i.m}{=} b_1(t)\sin \pi \mathrm{x} + \sum_{\substack{j=3 \\ odd}}^{\infty} b_j(t)\sin j\pi \mathrm{x} \qquad 3.15$$

Now that we have the approximate solution for the governing equations, we can solve for the analytical POD modes. The averaged autocorrelation function or the kernel is

$$R(x,x') = \sum_j^N \sum_k^N b_{jk}\sin j\pi \mathrm{x} \sin \mathrm{k}\pi \mathrm{x}' \qquad 3.16$$

which is ,by definition, separable and symmetric. Plugging (3.16) into the integral equation gives

$$\lambda\varphi(x) = \sum_{j}^{N}\sum_{k}^{N} b_{jk} \sin j\pi x \int_{0}^{1} \sin k\pi x' \, \varphi(x')dx' \qquad 3.17$$

Let $c_k = \int_0^1 \sin k\pi x' \, \varphi(x')dx'$ and taking the inner product of both sides of eq. (3.17) with $\sin i\pi x$ yields

$$\lambda \int_{0}^{1} \varphi(x) \sin i\pi x \, dx = \sum_{j}^{N}\sum_{k}^{N} b_{jk} \int_{0}^{1} \sin j\pi x \sin i\pi x \, dx \qquad 3.18$$

Letting $c_i = \int_0^1 \varphi(x) \sin i\pi x \, dx$ and the orthogonality of the sine functions reduces eq. (3.18) to

$$\lambda c_i = \frac{1}{2}\sum_{k=1}^{N} b_{ik} \, c_k \qquad 3.19$$

The eigenvectors $\{c_i\}$ are used to construct the orthonormal POD basis set as a

$$\varphi_i(\boldsymbol{x}) = \sum_{j=1}^{N} c_{j,i}\psi_j(x) = \sum_{j=1}^{N} c_{j,i} \sin j\pi x \qquad 3.20$$

where $c_{j,i}$ is the ith component of c_j. The new solution $w(t,x)$ for eq. (3.1) is now approximated by a linear combination of the POD basis functions as

$$w(t,x) \approx \sum_{i=1}^{N} a_i(t)\varphi_i(x) \approx \sum_{i=1}^{N} a_i(t) \sum_{j=1}^{N} c_{i,j}\psi_j(x) \qquad 3.21$$

To find the coefficients $\{a_i\}$ of the POD model, just take the inner product of eq. (3.21) with the POD basis where $w(t,x)$ is defined as the full-order approximate solution (3.12).

$$\begin{aligned} a_i(t) &= \int_0^1 w(t,x)\varphi_i(x)\,dx \\ &= \sum_{\substack{j=1 \\ odd}}^{N} b_j(t) \sum_{m=1}^{N} c_{m,i} \int_0^1 \psi_j(x)\psi_m(x)dx \\ &= \sum_{\substack{j=1 \\ odd}}^{N} b_j(t)\, c_{j,i} \end{aligned} \qquad 3.22$$

The coefficients, $\{a_i\}$, are equal to the linear combination of the $\{b_j\}$ and the columns of the eigenvectors, c.

Another way to solve for the a_i's is to perform Galerkin projection on the governing equations and initial condition again with the newly obtained POD basis to create the state-space form $\dot{\alpha}(t) = A\alpha + Bu$, where

$$A_{i,k} = 2\varepsilon \left[\int_0^1 \varphi_i(x) \frac{\partial^2 \varphi_k(x)}{\partial x^2} dx \right] \qquad 3.23$$

$$B_{k,2} = 2\varepsilon \left[\frac{\partial \varphi_k(0)}{\partial x} \quad -\frac{\partial \varphi_k(1)}{\partial x} \right] \qquad 3.24$$

The first eight analytical POD modes obtained are shown in Figure 1. The POD modes found utilizing the method of snapshots are shown in Figure 2 for comparison. Figure 1 and Figure 2 are not completely identical but they both exhibit the same overall shape. Unlike the modes in Figure 2, the modes in Figure 1 return to zero at the end points. This is due to the modes depending on the sine functions which vanish at the endpoints.

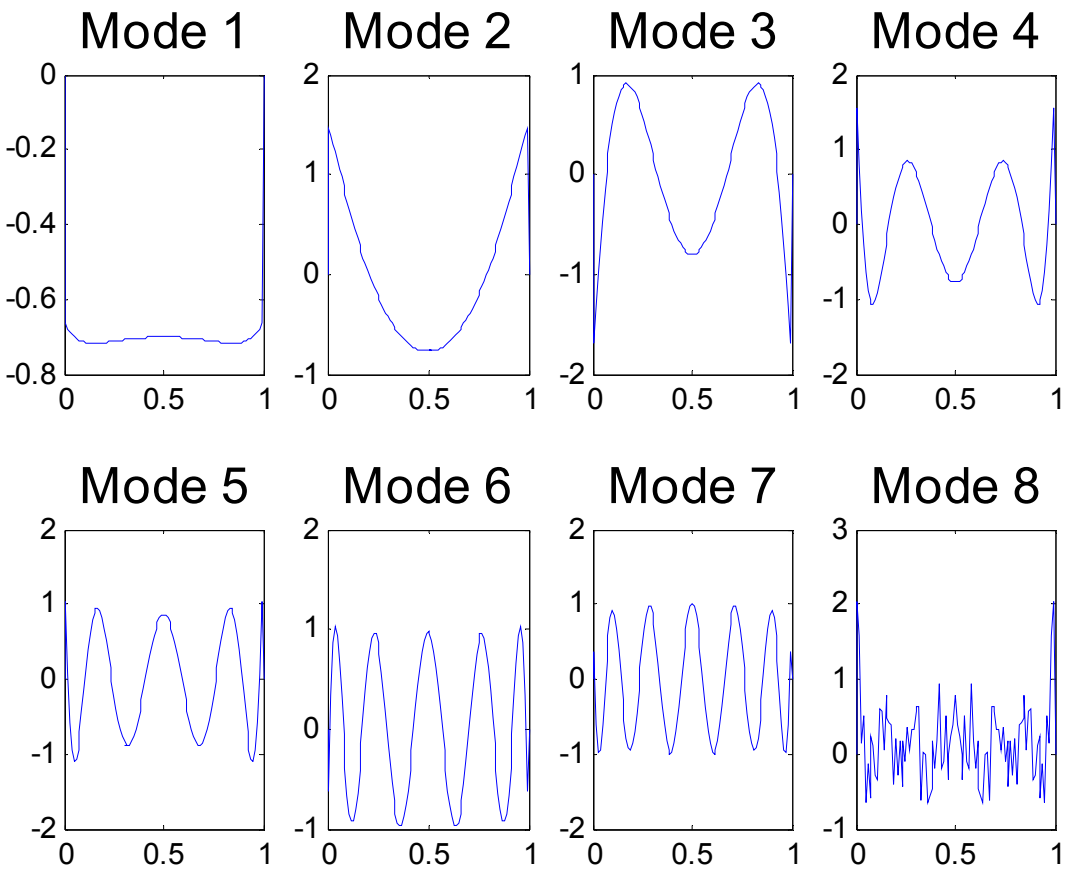


Figure 1. POD modes for the one-dimension problem

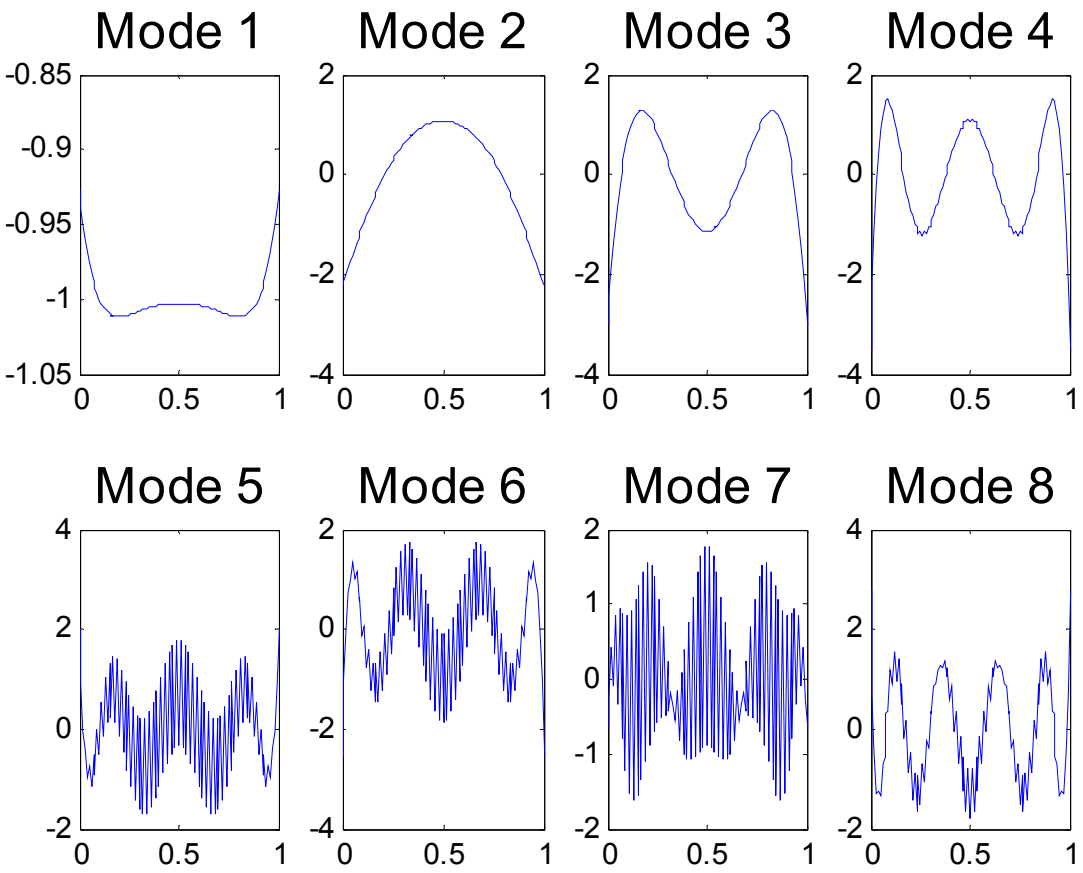


Figure 2. POD modes from method of snapshots

Before using the reduced-order model to develop feedback controls for the system, we verify that the results obtained from the reduced-order model and the full-order simulation are in good agreement. A condition that 99.9% of system energy must be captured was used for determining how many system modes were retained. This condition was met by a 30 POD basis modes. Although this is a major reduction from the numerical solution, it will be shown that important system dynamics can be retained with even lower state number models. The results are shown in Figure 3. In Figure 3, solid lines denote the solution of the full-order model and dashed lines represent solutions of the reduced-order model. The full-order model contained 500 states. In Figure 3, for the reduced-order model, instead of 30 POD modes we used 3 POD modes and, as is evident, very good agreement is seen between the reduced- and full-order simulations.

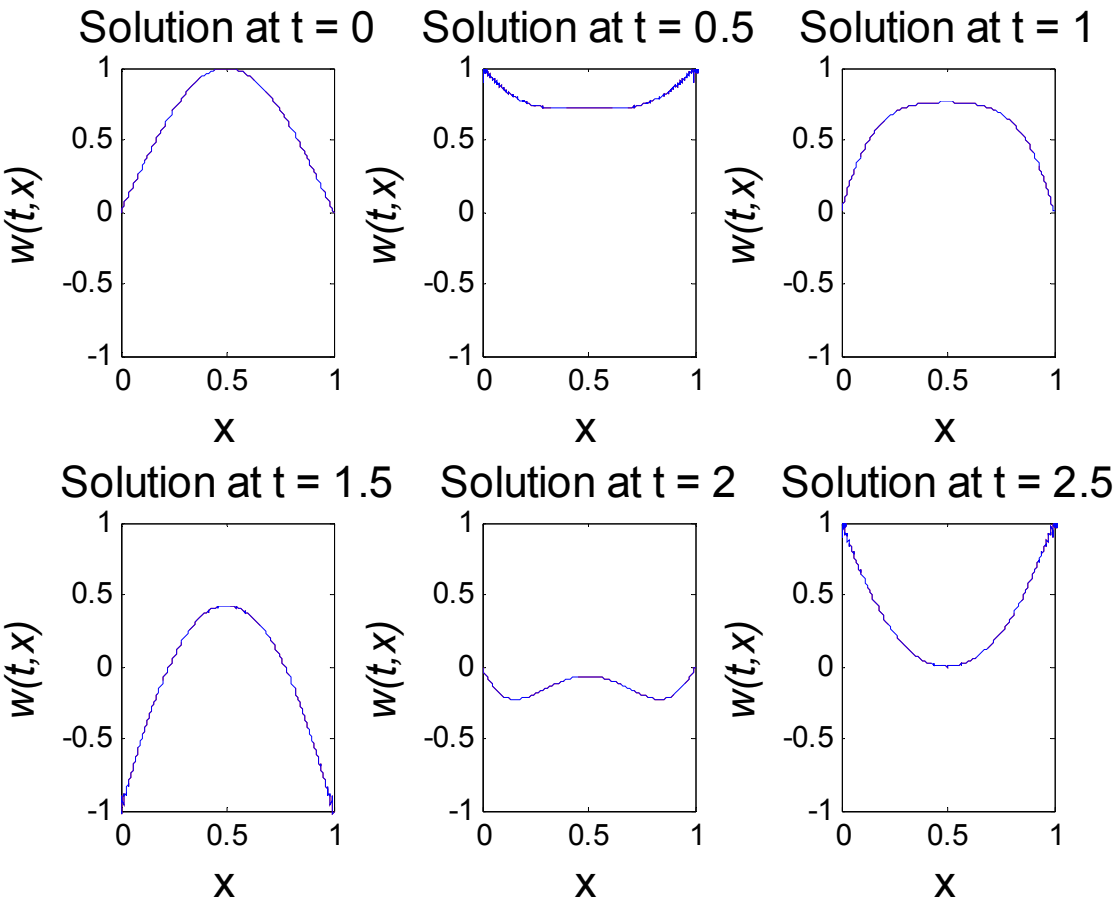


Figure 3. Model comparison for the one-dimension problem

For the one-dimensional case, many methods exist to either obtain an exact or approximate analytical solution for partial differential equation of many kinds and so analytic computation of the POD modes, most times, is possible. Figure 4 compares the temporal coefficients for the full-order model (blue) and the reduced-order model (red) using the analytical POD. The curves are coincident.

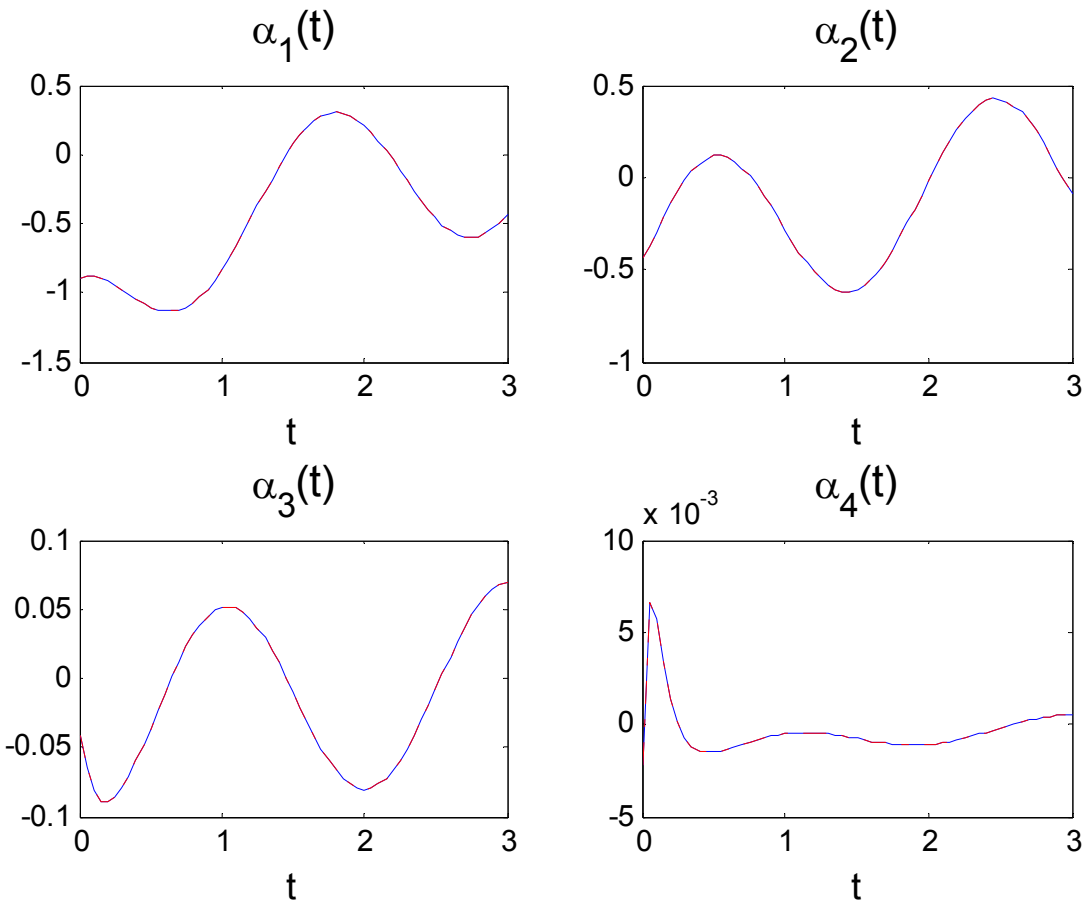


Figure 4. Comparison of full-order and analytical POD temporal coefficients

The Two-Dimensional Heat Equation

In this section we extend the techniques introduced in chapter 2 to a system described on a two-dimensional geometry, particularly a rectangular geometry. To develop the PDE model, the problem domain Ω is given by

$$\Omega = (0, a) \times (0, b) \qquad 3.25$$

where a and b are positive real-valued constants. The specific problem geometry considered is shown in Figure 5.

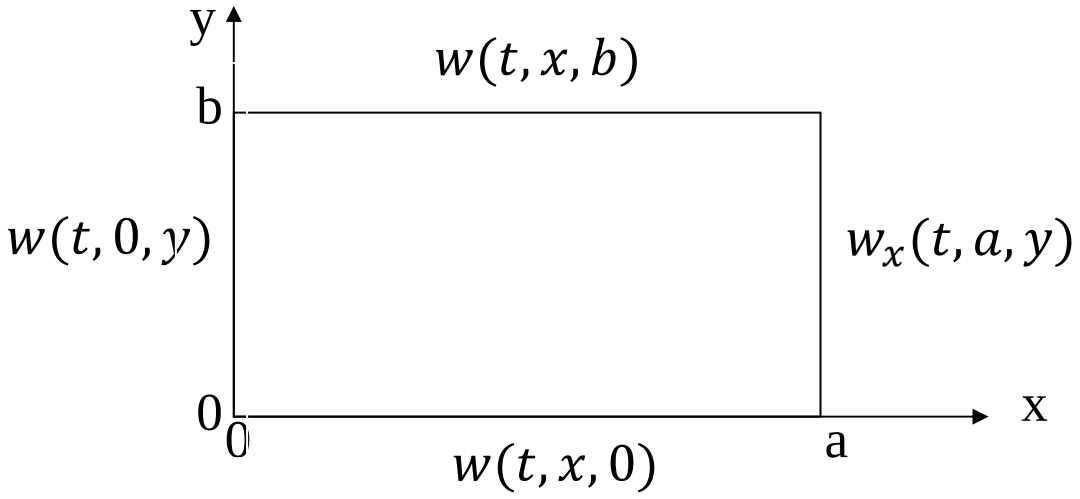


Figure 5. Two-Dimensional Problem Geometry

The two-dimensional heat equation is described by

$$w_t(t,x,y) = \varepsilon\left[w_{xx}(t,x,y) + w_{yy}(t,x,y)\right], \;\; t > 0, \;\; (x,y) \in \Omega \times \Omega \qquad 3.26$$

with initial conditions

$$w(0,x,y) = w_0(x,y) \in L^2(\Omega \times \Omega) \qquad 3.27$$

For this example, we specify Dirichlet boundary condition on the left, which is parabolic in nature, and a Neumann boundary condition equal to zero on the right side of the rectangle

$$w(t,0,y) = f(y) \qquad 3.28$$

$$w_x(t,a,y) = 0 \qquad 3.29$$

For simplicity, the boundary conditions on the top and bottom of the geometry are specified to be separable, that is, they are a product of a function of time and a function of the spatial variable and are described by the following functions

$$w(t,x,0) = u_B(t)\Phi_B(x) \qquad 3.30$$

$$w(t,x,b) = u_T(t)\Phi_T(x) \qquad 3.31$$

where $u_B(t)$ and $u_T(t)$ are the time-dependent controls and $\Psi_{\mathrm{B}}(\mathrm{y})$ and $\Psi_{\mathrm{T}}(\mathrm{y})$ describe the spatial effect of the controls. We assume that the solution to (3.26) be finite energy and can be approximated as a finite sum

$$w(t,x,y) = \sum_{i=1}^{N}\sum_{j=1}^{N} b_{ij}(t)\psi_{ij}(x,y) \qquad 3.32$$

where the $\{\psi_{ij}(x,y)\}$ are the known orthonormal basis functions and the $\{b_{ij}(t)\}$ functions the unknown temporal. As before, Galerkin projection can be performed

to completely define a set of ODEs for the $\{b_{ij}(t)\}$ coefficients.

In the results that follow, the initial condition specified is $w_0(x,y) = \sin\frac{\pi x}{a}\sin\frac{\pi y}{b}$. The constants are $a = 0.99$ and $b = 0.48$. The value for the conductivity constant is $\varepsilon = 0.1$. We chose the suitable basis functions to solve for the two-dimensional heat equation to be $\left\{\sin\frac{\mathrm{i}\pi\mathrm{x}}{\mathrm{a}}\sin\frac{\mathrm{j}\pi\mathrm{y}}{\mathrm{b}}\right\}_{\mathrm{i,j=1}}^{\mathrm{N}}$. The value for the control inputs are $u_B(t) = u_T(t) = \sin\pi t$ and the spatial functions are defined as $\Psi_{\mathrm{B}}(\mathrm{x}) = \Psi_{\mathrm{T}}(\mathrm{x}) = \sin\frac{\pi\mathrm{x}}{\mathrm{b}}$. First we simplify eq. (3.32) by making the following change of variable:

$$\beta_j(t) = \begin{bmatrix} b_{11}(t) \\ b_{12}(t) \\ \vdots \\ b_{ij}(t) \end{bmatrix}$$

$$\Phi_{\mathrm{j}}(\mathrm{x},\mathrm{y}) = \begin{bmatrix} \sin\pi x \sin\pi y \\ \sin\pi x \sin 2\pi y \\ \vdots \\ \sin i\pi x \sin j\pi y \end{bmatrix} \qquad 3.33$$

Now we can rewrite (3.32) as

$$w(t,x,y) \approx \sum_{j=1}^{N^2} \beta_j(t)\Phi_j(x,y) \qquad 3.34$$

Galerkin projection is performed and orthogonality of the basis functions creates the finite-dimensional model with state-space equations of the form

$$\begin{gathered} \dot{\beta}(t) = A\beta(t) + Bu + F \quad t > 0 \\ \beta(0) = b_o \end{gathered} \qquad 3.35$$

in terms of the $\{\beta_j\}$ where

$$A = -\varepsilon\left(\frac{i^2\pi^2}{a^2} + \frac{j^2\pi^2}{b^2}\right) \tag{3.36}$$

$$B = \begin{cases} \left[\frac{4j\pi\varepsilon}{2b^2} \quad -\frac{4j\pi\varepsilon}{2b^2}(-1)^j\right] & i = 1 \\ [0 \quad 0] & i > 1 \end{cases} \tag{3.37}$$

$$F = \begin{cases} \frac{4i\pi\varepsilon}{2a^2} & j = 1 \\ 0 & j > 1 \end{cases} \tag{3.38}$$

and b_0 is obtained by projecting the initial condition, w_0, onto the basis functions.

$$b_o = \begin{cases} 1 & i = 1, j = 1 \\ 0 & otherwise \end{cases} \tag{3.39}$$

Solving (3.35) – (3.39), we obtain a complete set of expressions that define the expansion coefficients for $w(t, x, y)$. Now, the averaged autocorrelation function for the two-dimension case is

$$R(x, x', y, y') = \sum_{j}^{N^2}\sum_{k}^{N^2} \beta_{jk}\, \Phi_j(x, y)\Phi_k(x', y') \tag{3.40}$$

which, by definition, is separable and symmetric. Plugging (3.40) into the two-dimensional integral equation (2.37) and following the steps outlined in chapter 2 yields

$$\lambda c_i = \frac{1}{2}\sum_{k=1}^{N^2} \beta_{ik}\, c_k \tag{3.41}$$

The orthonormal POD basis set is defined as

$$\varphi_i(x,y) = \sum_{j=1}^{N^2} c_{j,i}\Phi_j(x,y) \qquad 3.42$$

The new solution $w(t,x,y)$ for (3.34) is now approximated by a linear combination of the POD basis functions as

$$w(t,x,y) \approx \sum_{i=1}^{N^2} \alpha_j(t)\varphi_j(x,y) \qquad 3.43$$

The first eight analytical POD modes obtained are shown in Figure 6. Figures 7 and 8 show the full-order model and the reduced-order eight POD model, respectively.

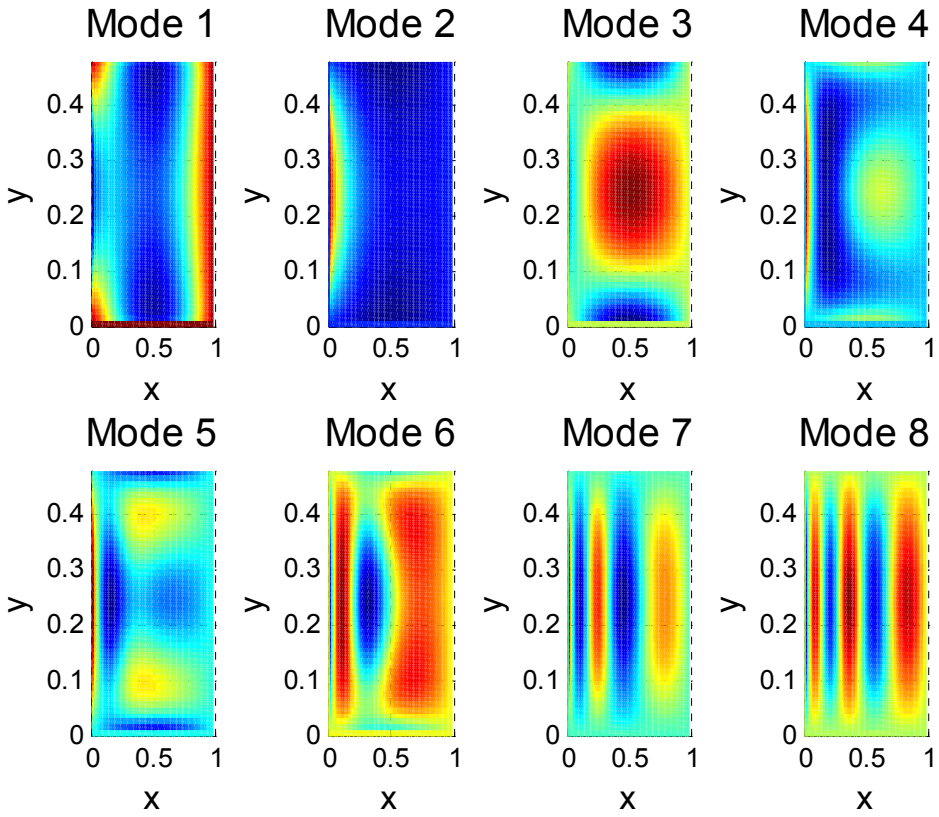


Figure 6. POD modes for the two-dimensional problem

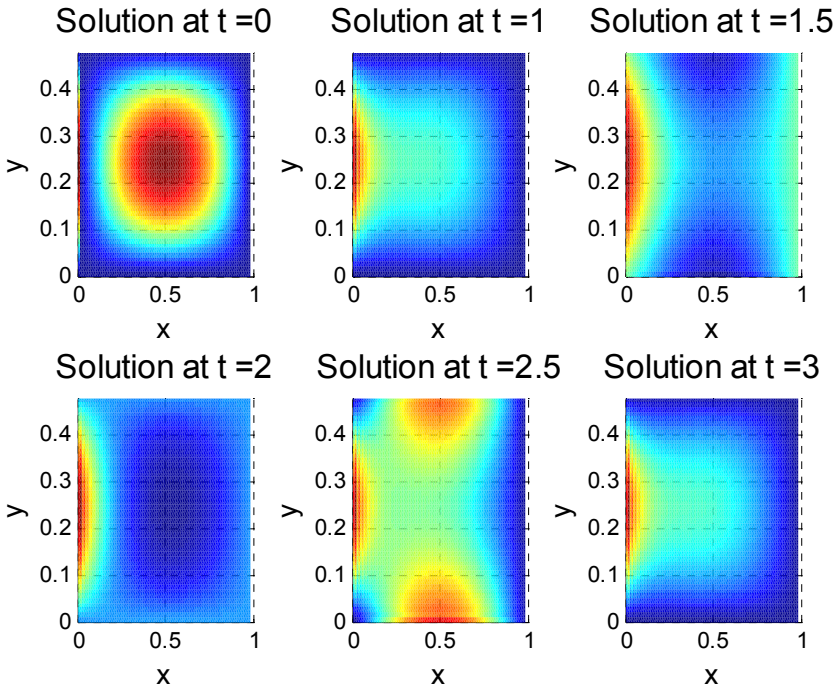


Figure 7. Full-order simulation

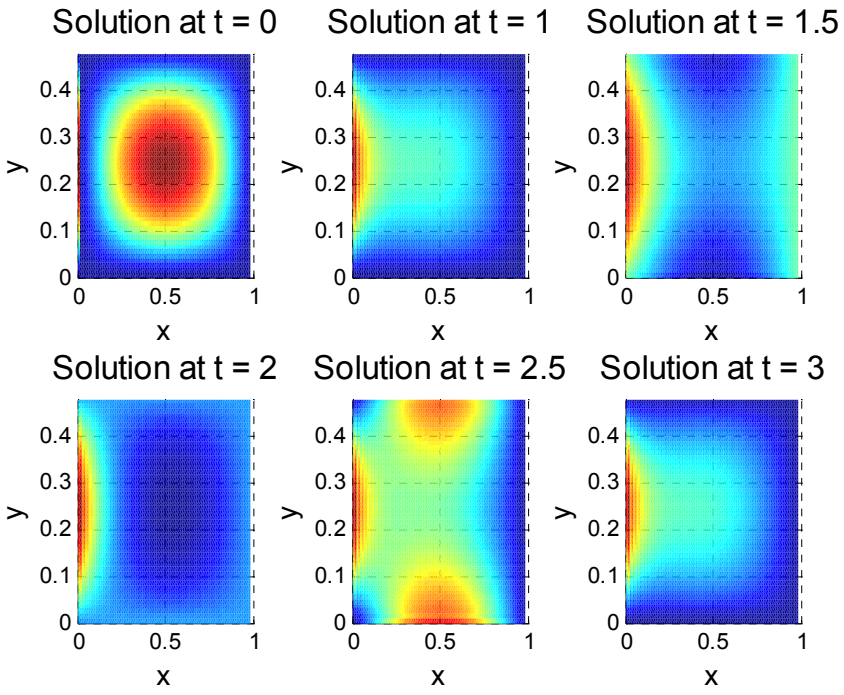


Figure 8. Reduced-order simulation

As is evident, the two Figures are indistinguishable. Another way to verify the results obtained from the reduced- and full-order models is to project the full-order solution at each time step onto the POD basis so to compare the temporal coefficients of each model. The temporal coefficients obtained for the first six modes are shown in Figure 9. In Figure 9, the solid curves denote projected coefficients while dashed curves represent coefficients from the reduced-order POD model. Very good agreement is seen between the reduced- and full-order simulations.

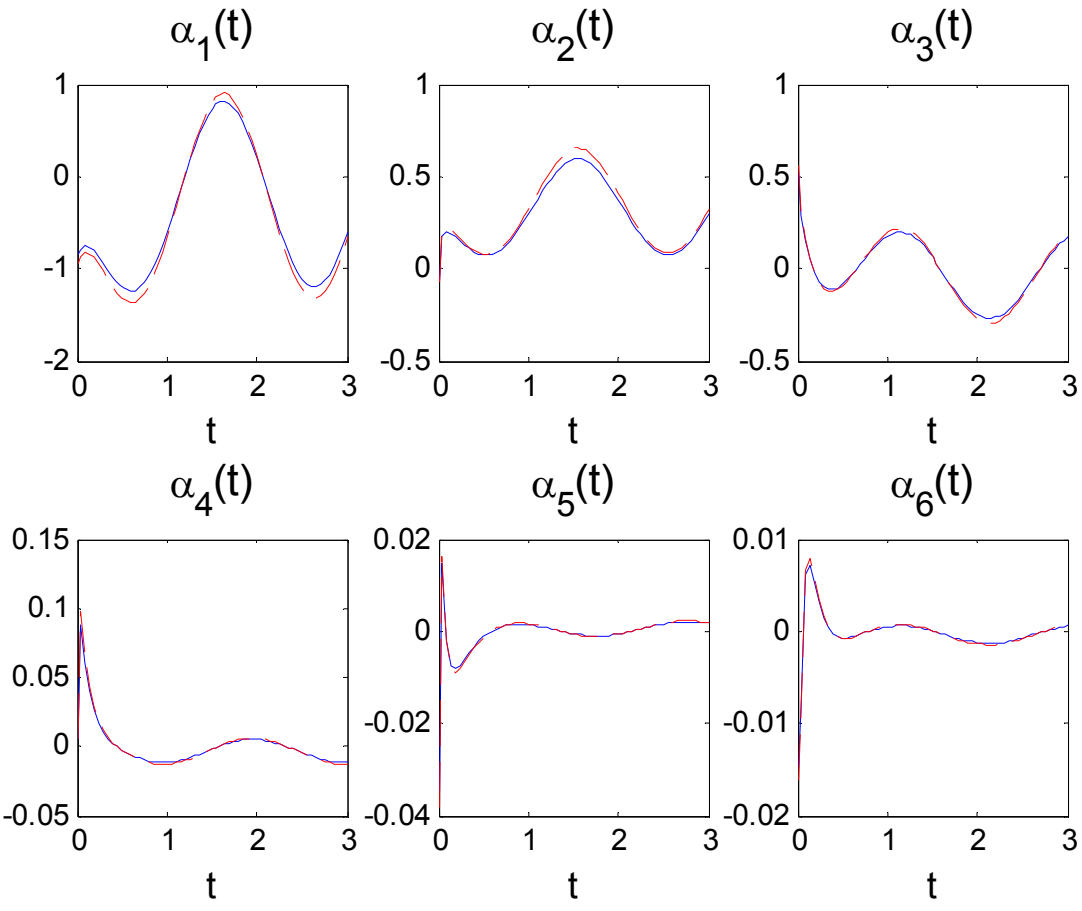


Figure 9. Projected and POD model coefficients

The techniques shown can be extended for more general problems with more defined boundary conditions. Most two-dimensional problems are easier when the domain shape is “regular” in some way. For example, PDE solution for a system whose domain is a rectangle or annulus is more readily available than for a problem in which the domain has an “amorphous” shape. Most approximate analytical methods, even the powerful Galerkin method, fail with complicated domains especially ones that introduce boundary singularities such as non-convex corners. If the problem geometry contains singularities, numerical simulation such as finite difference or finite element are necessary to gather data and proceed with the method of snapshots to obtain the POD basis. Despite this fact, there exists lots of literature on methods on how to rectify this problem for somewhat complex domains.

In this chapter, two prototype problems were given to illustrate the method for analytic computation of the POD basis and were compared to those obtained via the method of snapshots. Whether obtained analytical or numerical, proper orthogonal decomposition proves to be a powerful and effective method for model reduction. In the next chapter, we will demonstrate the effectiveness of using the reduced-order POD models for boundary control.

Chapter 4

Boundary Feedback Control

LQR Control Law Design

In many practical applications, boundary control is needed. The possibility of un-modeled dynamics in the system or dynamics lost in the model reduction process, makes feedback control a requirement [6]. As mentioned in chapter 1, there are two types of control of PDEs, in domain control where the actuation is evenly distributed everywhere in the domain or boundary control, where actuation is applied only through the boundary conditions. Boundary control of PDEs is generally considered more realistic, particularly those involved in fluids, because they can be actuated in a physically reasonable way only at the boundary, for example, feedback control of the air flow over the surface of an airplane wing. Boundary control is also generally considered to be the more difficult problem because it can lead to an unbounded input (B matrix) and output (C matrix) operator.

In this work, we are concerned with constructing boundary feedback control laws for finite-dimensional systems models with state-space equations of the form

$$\dot{\alpha}(t) = A\alpha + Bu, \qquad t > 0 \tag{4.1}$$

$$\alpha(0) = \alpha_0(x) \tag{4.2}$$

Equations (4.1-4.2) correspond to a linear system. However nonlinear partial differential equations result in nonlinear temporal models. Normally linearization is done resulting in a linear state-space equation of the form (4.1-4.2) to be used to design control laws for the nonlinear system [6].

In [6], boundary feedback control laws based on a linear quadratic regulator (LQR) methodology were developed from the weak formulation of the POD model system. We will use the techniques of that paper to develop the analytical POD control problem.

We consider the tracking problem for (4.1-4.2). A fixed reference signal $w_{ref}(x)$ is specified and projected onto the POD basis yielding tracking coefficients for the reduced-order model, denoted by a_{ref}. The dynamics of the system under tracking control are given by

$$\begin{bmatrix} \dot{a} \\ \dot{a_{ref}} \end{bmatrix} = \begin{bmatrix} A & 0 \\ 0 & 0 \end{bmatrix} \begin{bmatrix} a \\ a_{ref} \end{bmatrix} + \begin{bmatrix} B \\ 0 \end{bmatrix} u(t) = \bar{A}X + \bar{B}u \qquad 4.3$$

with a quadratic cost function defined as

$$J(w_0, u) = \int_0^\infty (a - a_{ref})^T Q(a - a_{ref}) + u^T R u \, dt \qquad 4.4$$

where Q is a diagonal, symmetric, positive semi-definite matrix of state weights and R is a diagonal, symmetric, positive definite matrix of control weights. The feedback control law that minimizes the cost is of the form [6]

$$\begin{aligned} u_{opt} &= -[K_1 \quad K_1]X \\ &= -[R^{-1}B^T P_1 \quad R^{-1}B^T P_2]X \end{aligned} \tag{4.5}$$

P_1 is the unique symmetric, nonnegative solution of algebraic Riccati equation

$$A^T P_1 + P_1 A - P_1 B R^{-1} B^T P_1 + Q = 0 \tag{4.6}$$

and P_2 in (4.5) satisfies the equation

$$[A^T - P_1 B R^{-1} B^T] P_2 = Q \tag{4.7}$$

Adding the optimal feedback control law, the resulting closed-loop system is of the form

$$\dot{X} = (\bar{A} - \bar{B}K)X \tag{4.8}$$

$$X(0) = X_0 \tag{4.9}$$

The tracking LQR formulation just discussed can be used to control the full-order model of the system as well as the reduced-order POD model with explicit control input.

In the infinite-dimensional setting of feedback control of partial differential equations feedback gain operators resulting from LQR control formulation can often be expressed in terms of an integral kernel called the functional gain. These functional gains, defined in (4.5) as K_1 and K_2, can indicate states most significant to the control and is an analogous idea to determine the relevant modes in the POD model to retain to that of the energy argument discussed in chapter 2.

Now with both the full-order model and the reduced-order POD model in hand, one can investigate the effectiveness of the LQR control strategy.

The One-Dimensional Heat Equation

We construct a tracking LQR boundary feedback control from the reduced-order analytical POD model found in chapter 3. The reference function $w_{ref}(x)$ is defined as [6]

$$w_{ref}(x) = 0.5x + 0.5 \tag{4.10}$$

We project the reference function onto the first three POD modes and the values obtained are used as tracking coefficients, a_{ref}, in the reduced-order control problem. We specify the control weight matrix R as the 2×2 identity matrix and the state weight 3×3 matrix Q is set to 1000. The behavior of the resulting closed-loop reduced-order model is illustrated in Figure 8. As seen in Figure 8, the reduced-order model, denoted by the solid blue line, consisting of only the first three modes tracks the reference signal, denoted by the red dashed line, and therefore it satisfies the control objective quite well.

For comparison, we apply the LQR technique to the full-order system. The resulting control problem is solved, and a full-order gain is obtained. The closed-loop behavior of the full-order system with full-order control is shown in Figure 10. The results of Figure 10 and Figure 11 are nearly the same. The reduced-order control provided by the three-mode POD model is able to track the reference signal as well as a full-order control via full state feedback, the best possible case.

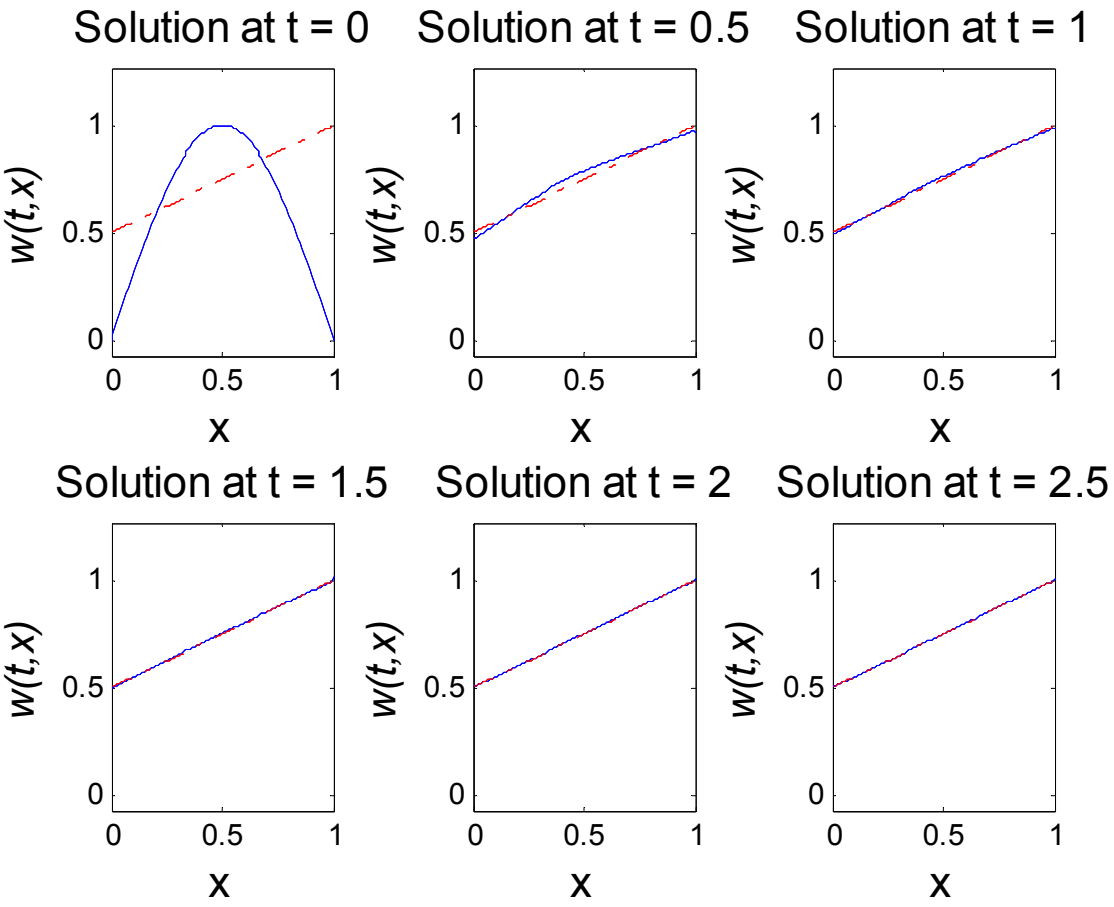


Figure 10. Controlled three-mode analytical POD model

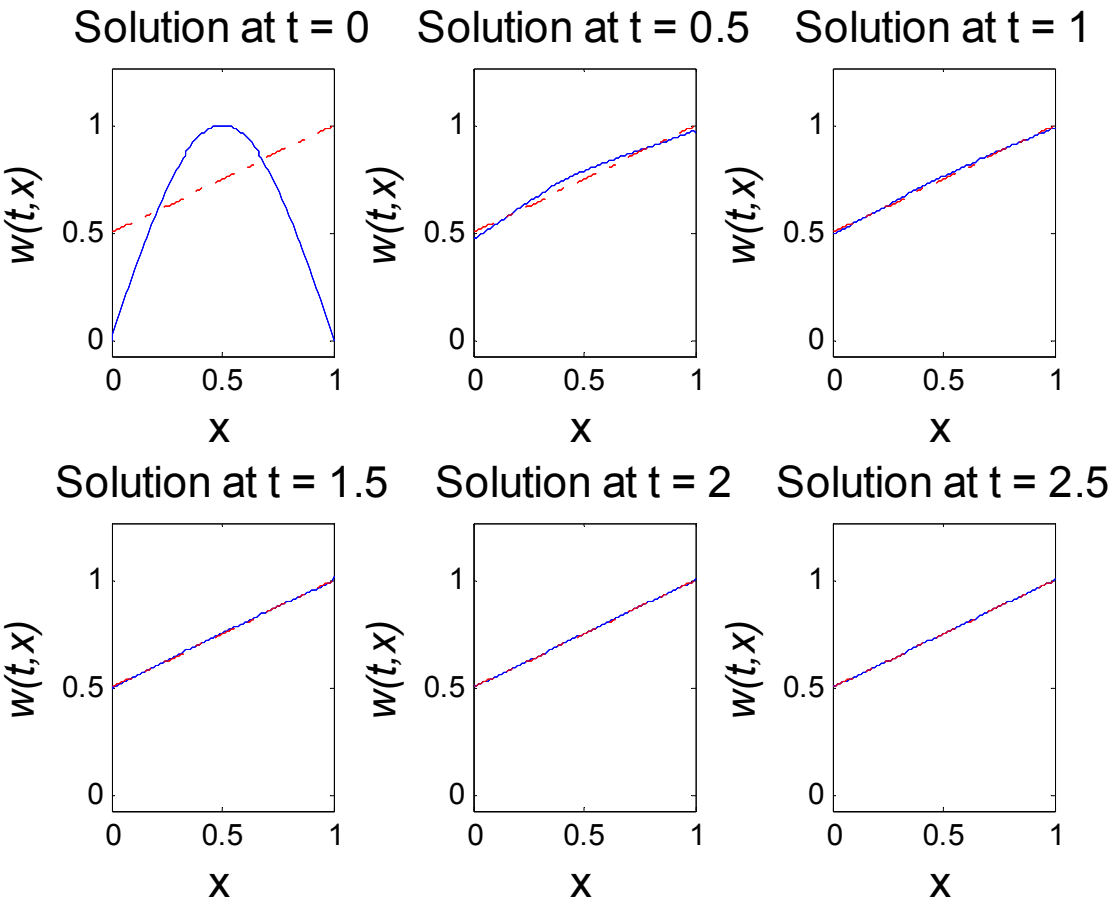


Figure 11. Full order Control

The Two-Dimensional Heat Equation

In this section, we utilize the reduced-order model found back in chapter 3 for tracking boundary feedback control. To construct a reference function in the results to follow, we specify a globally defined function $f(x, y)$ according

$$f(x,y) = \begin{cases} 0.5 & (x,y) \in [0,0.2] \times [0,0.48] \\ 0 & \text{otherwise} \end{cases} \quad 4.11$$

As before we project the reference function onto the first eight POD modes and the values obtained are used as tracking coefficients in the reduced-order control problem. We initially construct the control weight matrix R as the 2×2 identity matrix and the matrix of state weight as 8×8 matrix, Q. The first eight modes are given a state weight of 20000. The reference signal is shown in Figure 12. The behavior of the resulting closed-loop reduced-order model is illustrated in Figure 13. By comparing the controlled solution of Figure 13 with the reference signal shown in Figure 12, it is clear that the control objective is very closely achieved with a little error.

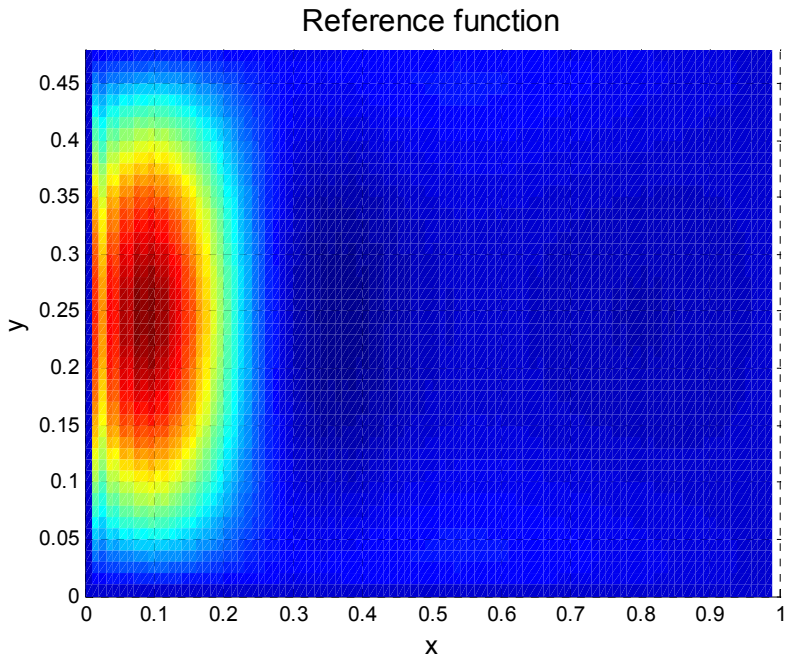


Figure 12. Reference function from a eight-mode projection

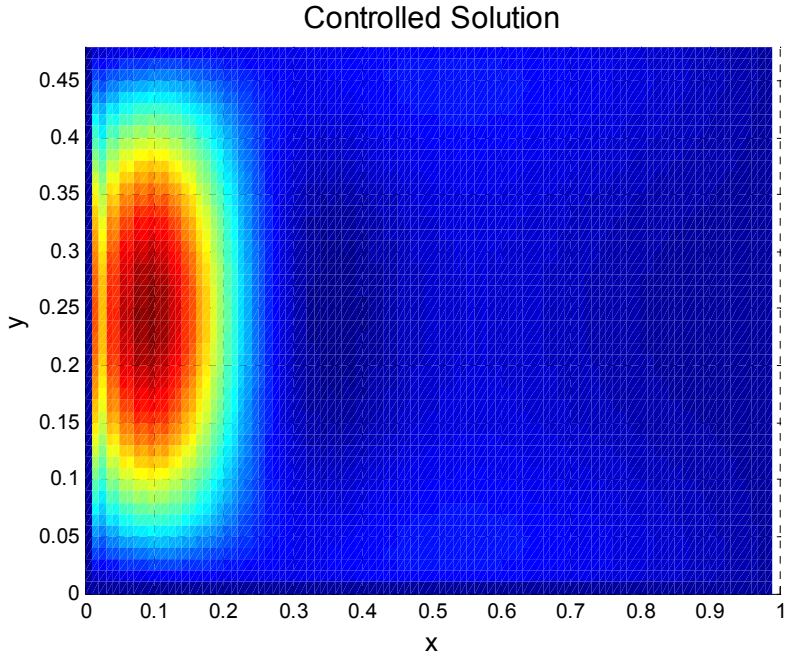


Figure 13. Steady-state controlled eight-mode POD model

In this chapter the effectiveness of boundary feedback controlled developed from analytical-based POD models has been demonstrated. Feedback controllers were obtained for reduced-order modes of the one- and two-dimension heat equation. In both examples, models consisting of eight modes or less were sufficient in developing effective control. The next chapter will introduce the idea of n-widths, how to approximate them and their uses.

Chapter 5

Model Reduction and N-Width Approximations

In model reduction we are interested in approximation by finite-dimensional models, and in particular, *n*-parameter affine models such as in POD. Model reduction can be broken down into two stages consisting of information acquisition and information processing. The first stage involves collecting information from an input-output experiment or simulation. The second stage involves obtaining a representation of available information [37]. Chapter 1 stated that model reduction should accurately and efficiently determine a reduced-order model with the least number of states possible while keeping the representation within a given error tolerance. This error can be split into two parts, the *inherent* and *representation* errors [37]. The inherent error is generated in the information collecting stage of simulation due to the lack of data and inaccurate measurements while the representation error is generated due to the loss of information in the information processing stage [10]. The optimal inherent and representation error can be quantified in terms of n-widths of various types. The analytic computation of the POD basis allows the explicit determination of the different optimal n-widths of the PDE solution $\mathrm{w}(\mathrm{t}, \mathbf{x})$.

First, $\mathrm{w}(\mathrm{t}, \mathbf{x})$ is viewed as the kernel in $L^2(\Omega)$ (Hilbert space) of a compact (integral) operator $\boldsymbol{W}$ defined as

$$\boldsymbol{W}: L^2(\Omega) \to L^2\big([0, \mathrm{T})\big) \tag{5.1}$$

$$(\boldsymbol{W}\phi)(t) \stackrel{\text{def}}{=} \int_{\Omega} w(t, \boldsymbol{x})\phi(\boldsymbol{x})d\boldsymbol{x} \tag{5.2}$$

Introduce the representation error of $\mathrm{w}(\mathrm{t}, \mathbf{x})$ as the optimal set distance between the range space of $\boldsymbol{W}$ and the finite-dimensional subspace X_n of $L^2([0, \mathrm{T}])$, i.e.,

$$dist\big(\boldsymbol{W}\big(L^2(\Omega)\big), X_n\big) = \sup_{\chi \in \boldsymbol{W}(L^2(\Omega))} \inf_{\eta \in X_n} \|\chi - \eta\|_2 \tag{5.3}$$

Thus (5.3) measures the extent to which the "worst element" of $\boldsymbol{W}$ can be approximated from X_n [27].

The minimal representation error of $w(t, \boldsymbol{x})$ by an n-dimensional subspace is given by

$$d_n\left(\boldsymbol{W}\big(L^2(\Omega)\big), L^2([0, \mathrm{T}])\right) \stackrel{\text{def}}{=} \inf_{X_n \in L^2([0,\mathrm{T}])} dist\big(\boldsymbol{W}\big(L^2(\Omega)\big), X_n\big) \tag{5.4}$$

This is exactly the Kolmogorov *n*-width of $\boldsymbol{W}\big(L^2(\Omega)\big)$ in $L^2([0, \mathrm{T}])$ [27]. If the infimum is attained for some subspace X_n, in $L^2([0, \mathrm{T}])$, we say that X_n is optimal. The optimal subspace gives the optimal n-dimensional affine model representing $w(t, \boldsymbol{x})$. The Kolmogorov n-width quantifies the representation error due to the inaccurate representation of the PDE solution $w(t, \boldsymbol{x})$. It represents the lost of information in the information processing stage. The inverse function of the Kolmogorov n-width d_n was called the metric dimension by Zames [34], which is

the dimension of the smallest subspace whose elements can approximate arbitrary points of $\boldsymbol{W}\left(L^2(\Omega)\right)$ to a specified tolerance. It can also be viewed as an approximate measure of the metric complexity of uncertain systems [37].

The operator $\boldsymbol{W}$ satisfies $(\boldsymbol{W}^*\boldsymbol{W})^{1/2}(\phi) = \boldsymbol{R}\phi$ where $\boldsymbol{R}$ is the integral operator with kernel, the autocorrelation function $R(\boldsymbol{x}, \boldsymbol{x}',)$.The singular values of the associated integral operator, $\boldsymbol{W}$, are defined as the square roots of the eigenvalues of the operator $\boldsymbol{W}^*\boldsymbol{W}$ where $\boldsymbol{W}^*$ is the adjoint of $\boldsymbol{W}$ given by

$$\boldsymbol{W}^*\boldsymbol{W}\phi_{\boldsymbol{i}} = \lambda_i\phi_i \tag{5.5}$$

where $\lambda_1 \geq \lambda_2 \geq \cdots > 0$. The $\{\lambda_i\}$ enumerate the nonzero eigenvalues associated with the operator $\boldsymbol{W}^*\boldsymbol{W}$ and $\{\phi_{\boldsymbol{i}}\}$ the associated orthonormal eigenvectors. Then the ith singular values of $\boldsymbol{W}$ is $\left\{\lambda_i^{1/2}\right\}$. The eigenvectors $\{\phi_{\boldsymbol{i}}\}$ are the POD modes of the corresponding PDE solution $w(t, \boldsymbol{x})$..Let us define the new functions $\{a_i\}$ as

$$a_i(t) = (\boldsymbol{W}\phi)(t) \stackrel{\text{def}}{=} \int_{\Omega} w(t, \boldsymbol{x})\phi(\boldsymbol{x})d\boldsymbol{x} \tag{5.6}$$

The functions $\{a_i\}$ are the eigenvectors of $\boldsymbol{W}^*\boldsymbol{W}$ therefore the “Hilbert-Schmidt” decomposition of kernel $w(t, \boldsymbol{x})$ is given by [10]

$$w(t, \boldsymbol{x}) = \sum_{i=1}^{N} a_i(t)\,\phi_i(\boldsymbol{x}) \tag{5.7}$$

where $\{a_i\}$ are the temporal coefficients and $\{\phi_{\boldsymbol{i}}\}$ are the POD basis. By Theorem 2.2 in [27] the Kolomogorov can be computed explicitly as

$$d_n\left(\boldsymbol{W}\left(L^2(\Omega)\right), L^2([0,\mathrm{T}])\right) \stackrel{\text{def}}{=} \lambda_{n+1}^{1/2} \tag{5.8}$$

Furthermore the optimal subspace is given by [35]

$$X_n = span\{a_1, a_2, \ldots a_n\} \tag{5.9}$$

where, we recall that

$$a_i = \int_{\Omega} w(t,\boldsymbol{x})\varphi_i(\boldsymbol{x})d\boldsymbol{x}, \quad i = 1,2,\ldots \tag{5.10}$$

are the temporal coefficients of the POD basis and they form a basis for $L^2([0,\mathrm{T}))$.

Introduce the notion of inherent error, we define δ^n as [34]

$$\delta^n \stackrel{\text{def}}{=} \sup\{\|\boldsymbol{W}\| : (\boldsymbol{W}u)(t) = 0, \forall t = t_1, \cdots, t_n\} \tag{5.11}$$

The time n-width is defined as [37]

$$\Theta^n\left(\boldsymbol{W}\left(L^2(\Omega)\right), L^2([0,\mathrm{T}])\right) \stackrel{\text{def}}{=} \inf_{u \in L^2(\Omega)} \delta^n(u) \tag{5.12}$$

The time n-width characterizes the time complexity of the data acquisition process. It is the best achievable inherent error with n consecutive snapshots. The inverse of the time n-width gives the least time needed to reduce the inherent error to any specified level. The inherent error is irreducible no matter what model reduction method is used in the second stage [37].

The n-width in the sense of Gel'fand, is defined as [27]

$$d^n\left(\boldsymbol{W}\left(L^2(\Omega)\right), L^2([0,\mathrm{T}])\right) = \inf_{Y^n} \sup_{\phi \in Y^n, \|\phi\|_2 \leq 1} \|\boldsymbol{W}\phi\|_2 \qquad 5.13$$

where the infimum is taken over all subspaces Y^n of $L^2(\Omega)$ of co-dimension at most n. A subspace is said to be of co-dimension n if there exist n-independent bounded linear functionals $\{\phi_i\} \in L^2(\Omega)$ such that [27]

$$Y^n = \{\phi \in L^2(\Omega), (\phi, \phi_i) = 0, i = 1, .., n\} \qquad 5.14$$

where $(\cdot,\cdot)$ denotes the inner product. If the infimum is achieved in the definition of d^n for some subspace Y^n then it is said to be optimal.

The Gel'fand n-width can be seen as the optimized inherent error based on n arbitray linear measurements, whereas in the case of the time n-width, the measurements are restricted to be n consecutive snapshots. The Gel'fand n-width characterizes the experimental complexity of the information collecting stage using simulation or identification. The inverse of the Gel'fand n-width gives the least number of measurements needed to reduce the error in approximating $w(t, \boldsymbol{x})$ to a predetermined value [37]. By Theorem 2.2 in [27] the Gel'fand n-width can be explicitly computed as

$$d^n\left(\boldsymbol{W}\left(L^2(\Omega)\right), L^2([0,\mathrm{T}])\right) \stackrel{\text{def}}{=} \lambda_{n+1}^{1/2} \qquad 5.15$$

and the optimal subspace of co-dimension n as (5.14) where $\{\phi_i\}$ are the POD basis. The optimal subspace of co-dimension n can be computed as [35]

$$Y^n = \{\phi \in L^2(\Omega), (\phi, \phi_i) = 0, i = 1, .., n\} \qquad 5.16$$

where $\{\phi_i\}$ is the POD basis.

The linear n-width is defined by

$$\delta_n\left(\boldsymbol{W}\left(L^2(\Omega)\right), L^2([0,\mathrm{T}])\right) = \inf_{P_n} \sup_{\phi\in L^2(\Omega),\|\phi\|_2\leq 1} \|\boldsymbol{W}\phi - P_n\phi\|_2 \qquad 5.17$$

where P_n is any continuos linear operator from $L^2(\Omega)$ into $L^2([0,\mathrm{T}])$ of rank at most n. If the infimum is achieved in the definition of δ_n then the linear operator $P_n\phi = \sum_{i=1}^{N}(\phi,\phi_i)a_i$ it is said to be optimal. For the solution of the heat equation the linear n-width can also be explicitly computed as

$$\delta_n\left(\boldsymbol{W}\left(L^2(\Omega)\right), L^2([0,\mathrm{T}])\right) \stackrel{\text{def}}{=} \lambda_{n+1}^{1/2} \qquad 5.18$$

Finally, the n-width in the sense of Bernstein of $w(t,\boldsymbol{x})$ is defined as the Bernstein n-width of $\boldsymbol{W}\left(L^2(\Omega)\right)$ defined by [27]

$$b_n\left(\boldsymbol{W}\left(L^2(\Omega)\right), L^2([0,\mathrm{T}])\right) \stackrel{\text{def}}{=} \sup_{X_{n+1}} \sup\{\beta : \beta S(X_{n+1}) \subseteq L^2([0,\mathrm{T}])\} \qquad 5.19$$

where X_{n+1} is any $(n+1)$-dimensional subspace of $L^2([0,\mathrm{T}])$ and $S(X_{n+1})$ is the unit ball in X_{n+1}, that is,

$$S(X_{n+1}) = \{y \in X_{n+1} : \|y\|_2 \leq 1\} \qquad 5.20$$

An optimal subspace is a subspace for which the supremum in the definition is achieved. For the solution of the heat equation the Bernstein *n*-width can also be explicitly computed as [35]

$$b_n\left(\boldsymbol{W}\left(L^2(\Omega)\right), L^2([0,\mathrm{T}])\right) \stackrel{\text{def}}{=} \lambda_{n+1}^{1/2} \qquad 5.21$$

and the optimal subspace is given by [35]

$$X_{n+1} = span\{a_1, a_2, \dots a_{n+1}\} \quad 5.22$$

Theorem 2.2 from [27] results in a way to calculate the n-widths to give us explicit optimal subspaces and operators. The goal of POD is to approximate the solution of the PDE with linear superposition of n basis functions $\{\phi_i\}_{i=1}^{N}$. Overall, some sets of basis functions are better than others, optimizing the n-widths results in finding the *best* basis functions available and the error they achieve.

In this chapter we discussed the different kind of n-widths available, how they are obtained and their relevance to the POD. It was also discussed how the n-widths can be utilized to describe the metric complexity of the models. The final chapter will conclude this thesis and talk about future work.

Chapter 6

Conclusion and Future Work

The goal of model reduction is to find a low-dimensional approximation for a high-dimensional system while preserving the input-output behavior. In the case of partial differential equations, it is essential to make the system model solution tractable. Several model reduction methods exist such as Krylov-subspace, Hankel-norm, balanced truncation, and of course proper orthogonal decomposition. In this thesis, we focused on POD and derived the POD modes explicitly for the one- and two-dimensional heat equations with boundary controls inputs. The POD modes are the solutions to the Fredholm integral equations of the second kind with the kernel equal to the averaged autocorrelation function found from the approximate solution of the partial differential equation. The analytic POD modes were compared to the empirical POD modes obtained from using the method of snapshots which exhibited a close match. The choice to use only eight POD basis vectors for the reduced-order models of both the one-dimensional and two-dimensional heat equation was made since these eight modes were sufficient to capture more than 99.9% of the total energy. Furthermore, these 8^{th} order POD models matched their full-order simulations very closely. The limitation of obtaining these analytic POD modes depends on the availability of an exact or approximate analytic solution to the PDE. Most analytic methods fail with the choice of the geometry. Any boundary singularities

within the geometry make finding an exact solution either complex or impossible. In this case one would have to rely on the method of snapshots to find the POD vectors. Despite the choice of either the empirical or analytical POD vectors, POD has been shown to be a powerful and effective method for model order reduction.

With the reduced-order POD model, we investigated the effectiveness of the LQR control by implementing the control in the reduced-order model. A Dirichlet boundary LQR controller was designed for the reduced-order model using only eight POD modes and achieved tracking for the one-dimensional and two-dimensional heat equation. For the one-dimension case, the controlled 8^{th} order POD was compared to the controlled full-order model and they were indistinguishable. These results prove the effectiveness of POD in the application of boundary feedback control of PDEs where control design of the full-order system is an intractable problem.

Additionally, the idea that model reduction could be split into two stages and formulated as an input design and model selection problem was introduced in chapter 5. Recall that the goal of POD is to approximate the solution of the PDE with linear superposition of n basis functions $\{\phi_i\}_{i=1}^{N}$. It was shown that the analytic determination of the POD modes for the heat equation allows the computation of various n-widths explicitly. Optimizing these different n-widths

resulted in finding the *optimal* basis functions (POD modes) available and the error they achieved. This error consisted of the inherent and representation error achieved. It was latter shown that these various n-widths characterized the reduced-order models obtained using POD modes for the heat equation.

Much of the research today is in the area of model reduction of nonlinear partial differential equations such as the Burgers' equations or the Navier-Stokes equations. The general framework for model reduction of these systems is projection-based like POD, which is a linear process. A different approach would be to think of the solutions to these nonlinear PDE systems as belonging to manifolds. POD has been used to describe such systems but is limited in that it only works for data lying in a Euclidian vector space. While this is certainly sufficient, as we have seen [2][9][12][13], for certain models it does not handle more complex representations particularly manifolds. Some work has been done to develop a method of principal geodesic analysis (PGA) for the manifold setting [38]. Points far apart on the underlying manifold, as measured by their geodesic distance, may appear close in the high-dimensional space, as measured by their straight-line Euclidian distance [36]. The geodesic distance reflects the low-dimensional geometry of the manifold, unlike PCA (POD). Popular manifold learning programs such as ISOMAP build on PCA by describing the variability of data on a manifold [36]. ISOMAP is one of several widely used low-dimensional embedding methods, where geodesic distances on a weighted graph are

incorporated with the classical scaling [36]. Favorable results might be expanded via this method and others LLE [39] for model reduction of nonlinear PDEs.

List of References

[1] Willcox, K. and Peraire, J., Balanced Model Reduction via the Proper Orthogonal Decomposition, AIAA, Vol. 40, No. 11, November 2002, pp. 2323-2330.

[2] Camphouse, Chris R. and James H. Myatt, “Reduced Order Modeling and Boundary Feedback Control of Nonlinear Convection”, AIAA Guidance, Navigation, and Control Conference, 2005.

[3] Efe, M. O. And Ozbay H., “Proper Orthogonal Decomposition for Reduced Order Modeling: 2D Heat Flow”, IEEE, 2003.

[4] Holmes, P., Lumley, J. L., Berkooz, G., *Turbulence, Coherent Structures, Dynamical Systems and Symmetry*, Cambridge University Press, 1996.

[5] Camphouse, R. C., Djouadi, S. M., and Myatt, J. H., “Feedback Control for Aerodynamics”. IEEE Conference on Decision and Control, Dec 2006.

[6] Camphouse, R. C., “Boundary Feedback Control Using Proper Orthogonal Decomposition Models”, Journal of Guidance, Control, and Dynamics, vol 28, no 5, September-October, 2005.

[7] Caraballo, E., Samimy, M., and DeBonis, J., “Low Dimensional Modeling of Flow for Closed-Loop Flow Control,” AIAA Paper 2003-0059, January 2003.

[8] Carlson, H., Glauser, M., Higuchi, H., and Young, M., POD Based Experimental Flow Control on a NACA-4412 Airfoil, AIAA Paper 2004-0575, January 2004.

[9] Camphouse, R.C. and Myatt, J.H., “Feedback Control for a Two-Dimensional Burgers’ Equation System Model”, AIAA Paper 2004-2411, June 2004

[10] Djouadi, S.M., On the Optimality of the Proper Orthogonal Decomposition and Balanced Truncation, Proceedings of the 47th IEEE Conference on Decision and Control, Cancun, Mexico, December 2008, pp. 4221- 4226.

[11] Ilak, M. and Rowley, C. W., Modeling of Transitional Channel Flow Using Balanced Proper Orthogonal Decomposition, Physics of Fluids 20(034103), March 2008.

[12] Djouadi, S. M., Camphouse R.C., and Myatt, J.H., Empirical Reduced-Order Modeling for Boundary Feedback Flow Control, Journal of Control Science and Engineering Volume 2008 (2008), Article ID 154956, 11 pages.doi:10.1155/2008/154956.

[13] Fernandez, T., Djouadi, S.M., and Foster, J., Empirical Hankel Norm Model Reduction with Application to a Prototype Nonlinear Convective Flow

[14] Glover, K., “All Optimal Hankel-norm Approximations of Linear Multivariable Systems and their L^{∞}-error Bounds”, International Journal of Control, 39:6, 1115 – 1193. 1984.

[15] Kung, S. Y., “Optimal Hankel-norm Model Reductions: Scaler Systems,” in Proceedings 1980 Joint Automatic Controls Conferenece., San Francisco, CA, Paper FA8.A, August 1980.

[16] Kung, S. Y., and Lin, D. W., “Optimal Hankel-norm Model Reductions: Multivariable Systems,” IEEE Transactions on Automatic Control, vol. 26, pp. 832-852, 1981.

[17] Schatten R. Norm Ideals of Completely Continuous Operators, Springer-Verlag, Berlin, Gottingen, Heidelberg, 1960.

[18] Riesz, F., and Nagy, B. Sz., *Functional Analysis*, Dover, 1990.

[19] Kanwal, R.M., *Linear Integral Equations: Theory and Technique*, Academic Press, 1971.

[20] Baker A.J., *The Computational Engineering Sciences*, j-Computek Press, Loudon TN, 2007, 267 pages + DVD.

[21] Porter, D., and Stirling, D., *Integral Equations: A Practical Treatment, from Spectral Theory to Applications*, Cambridge University Press, 1990.

[22] Strauss, W., *Partial Differential Equations: An Introduction*, John Wiley and Sons, Inc., 2008.

[23] Zhou, K., Doyle, J.C., and Glover, K., *Robust and Optimal Control*, Prentice Hall, 1996

[24] Rugh, W.J., *Linear System Theory*, Prentice Hall, Second Edition, 1996

[25] Schatten R., *Norm Ideals of Completely Continuous Operators*, Springer-Verlag, Berlin, Gottingen, Heidelberg, 1960.

[26] Camphouse, R.C., Basis Construction for the Design of Boundary Feedback Controls from Reduced Order Models.

[27] Pinkus, A., n*-Widths in Approximation Theory*, Springer-Verlag, 1985.

[28] Kosambi, D. D., Statistics in Function Space. *J. Inidian Math. Soc*., 7:76-88. 1943.

[29] Loéve, M., Functions Aleatoire de Second Order. *Comptes Rendus Acad. Sci. Paris,* 220, 1945.

[30] Karhunen, K., Zur Spektraltheorie Stochastischer Prozesse. *Ann. Acad. Sci. Fennicae,* Ser. A1, 34, 1946.

[31] Cusumano, J.P., Sharkady, M. T., and Kimble, B.W., *Philos. Trans. R. Soc. London,* Ser. A, 1994, 347, 421-438.

[32] Jolliffe, I.T., *Principle Component Analysis*, Springer-Verlag, 2002

[33] Sirovich, L. and Rodriguez, J.D., Coherent Structures and Chaos: A Model Problem. *Phys. Lett. A,* 120(5):211-14, 1987.

[34] Zames, G., Lin, L., and Wang, L.Y., Fast-Identification n-widths and Uncertainty Principles for LTI and Slowly Varying Systems. *IEEE Transactions on Automatic Control*, Vol. 39, No. 9, 1994.

[35] Fernandez, T. Djouadi, S. M., and Camphouse, R.C., “Analytical Computation of Proper Orthogonal Decomposition Modes and n-Width Approximations for the Heat Equation with Boundary Control.” To apprear at 49th IEEE Conference on Decision and Control. 2010.

[36] Tenenbaum, J.B., de Silva, V., and Langford, J.C., A Global Geometric Framework for Nonlinear Dimensionality Reduction, Science, Vol. 29, 2000.

[37] Djouadi, S.M., On the Connection Between Model Reduction and N-widths Approximation. SIAM Annual Meeting and SIAM Conference on Life Sciences. Pittsburgh, PA. July 2010.

[38] Fletcher, P.T., Lu, C., Pizer, S.M., and Joshi, S. Principle Geodesic Analysis for the Study of Nonlinear Statistics of Shape. IEEE Transactions on Medical Imaging

[39] Roweis, S.T., and Saul, L.K. Nonlinear Dimensionality Reduction by Locally Linear Embedding. Sciecne 22. Vol 290., No. 5500. pp. 2323-2326. 2000.

Vita

Tasha Fernandez was born in New Orleans, Louisiana. She moved to Memphis, Tennessee when she was 12 years old. After graduating from Craigmont High School, she went to the University of Tennessee at Knoxville (UTK) where she studied Electrical Engineering. Then after graduating with a Bachelor of Science degree in Electrical Engineering, she took a year off to travel abroad. She returned to the University of Tennessee to begin her graduate studies. She also worked for the summer at Oak Ridge National Laboratory (ORNL) as a Research Alliance in Math and Science (RAMS) student. She graduated from the University of Tennessee with a Master of Science degree in Electrical Engineering in 2010.